INL/EXT-13-28031

In-Vessel Coil Material Failure Rate Estimates for ITER Design Use

L. C. Cadwallader

January 2013

The INL is a U.S. Department of Energy National Laboratory
operated by Battelle Energy Alliance

INL/EXT-13-28031

In-Vessel Coil Material Failure Rate Estimates for ITER Design Use

L. C. Cadwallader

January 2013

Idaho National Laboratory
Experimental Programs
Idaho Falls, Idaho 83415

http://www.inl.gov

Prepared for the
U.S. Department of Energy
Office of Nuclear Energy
Under DOE Idaho Operations Office
Contract DE-AC07-05ID14517

ABSTRACT

The ITER International Project design teams are working to produce an engineering design for construction of a large tokamak fusion experiment. One of the design issues is ensuring proper control of the fusion plasma. In-vessel magnet coils may be needed for plasma control, especially the control of edge localized modes and plasma vertical stabilization. These coils will be lifetime components that reside inside the ITER vacuum vessel behind the blanket modules. As such, their reliability is an important design issue because access will be time-consuming if any type of repair is necessary. This report gives the research results and estimates of failure rates for the coil conductor and jacket materials to be used for the in-vessel coils. Copper and CuCrZr conductors as well as stainless steel and Inconel jackets are examined.

CONTENTS

TABLES

FIGURES

NOMENCLATURE

AF	acceleration factor
API	American Petroleum Institute
cfu	colony-forming unit
CuCrZr	Copper Chromium Zirconium alloy
D-D	deuterium-deuterium
D-T	deuterium-tritium
dpa	displacements per atom
EBR-II	Experimental Breeder Reactor-II
ELM	edge localized mode
ITER	the ITER International Project (iter is latin for the way)
IVC	in-vessel coil
MIC	microbiologically influenced corrosion
NASA	National Aeronautics and Space Administration
NRC	U.S. Nuclear Regulatory Commission
ppb	parts per billion
rms	root mean square
SL-2	seismic level 2
TF	toroidal field
TFTR	Tokamak Fusion Test Reactor
TPL	toroidal pumped limiter
UNS	Unified Numbering System for alloys
VS	vertical stabilization

SYMBOLS

A	acceleration in vibration
AF	acceleration factor for failure rate modification
χ^2	Chi-square factor for Chi-square statistical distribution
Δ	radiation degradation factor
D	diffusion coefficient
D	peak displacement in vibration
d_H	hydraulic diameter of a pipe
E_n	neutron energy
f	frequency in hertz
g	gravities
k	mass transfer effect
k	failure rate modifier factor
λ	failure rate
n	number of failure events
P	wetted perimeter
P_o	a characteristic parameter of the material before radiation exposure
P_t	a characteristic parameter of the material after total radiation dose
P_f	a characteristic parameter of the material at failure
r	minor radius of a tokamak
R	major radius of a tokamak
Re	Reynolds number
Sc	Schimdt number
Sh	Sherwood number
T	temperature
T	total operating time, usually in hours
t	tube or pipe wall thickness
ν	kinematic viscosity of fluid

In-Vessel Coil Material Failure Rate Estimates for ITER Design Use

1. Introduction

The ITER International Project design teams are working to produce an engineering design for construction of a large tokamak fusion experiment. One of the design issues is ensuring proper control of the fusion plasma. In-vessel magnet coils may be needed for plasma control, especially the control of edge localized modes (ELMs) and plasma vertical stabilization (VS). These coils will be lifetime components that reside inside the ITER vacuum vessel behind the blanket modules. As such, their reliability is an important design issue because access will be time-consuming if any type of repair is necessary.

This report gives failure rate estimates for the coil materials for the ITER in-vessel coils (IVCs). The proposed IVCs will be jacketed resistive magnet coils with magnesium oxide insulated hollow conductor (Neumeyer et al. 2011). This mineral insulated conductor design has been shown to withstand high radiation exposure in other applications, so it is considered to be an enabling technology for ITER IVCs that will also have high radiation exposure over the coil lifetime.

There are two subsystems of IVCs: the coils for plasma VS and the coils for plasma ELM control. The VS coils are copper conductor with a stainless steel jacket and the ELM coils are CuCrZr conductor with an Inconel jacket. The ELM coils have 6 turns and 15 kA per turn; the conductor is about 6 m per turn. The VS coils have 4 turns and a peak coil current of 60 kA. The preliminary VS and ELM designs are shown in Figure 1 and Figure 2, respectively (Heitzenroeder 2012a). Water flows in the hollow conductor for cooling.

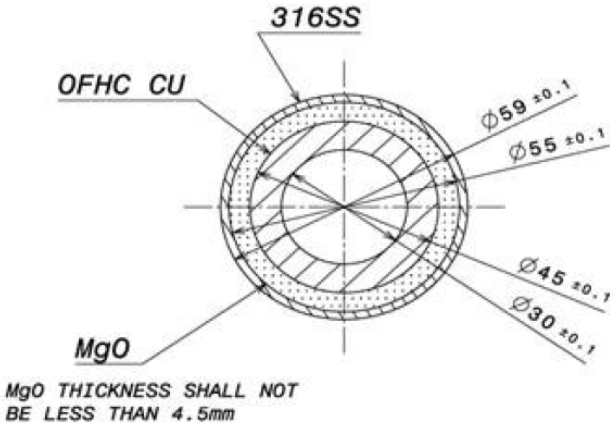

Figure 1. Vertical stabilization coil preliminary configuration

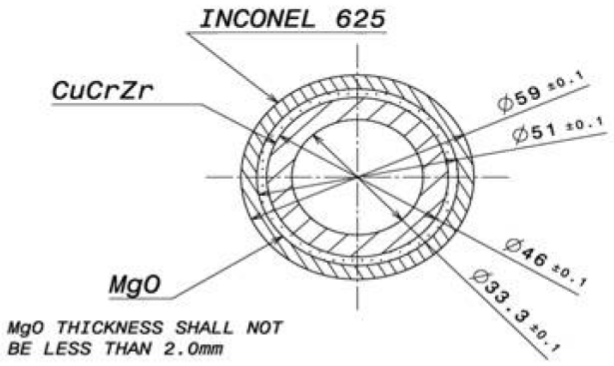

Figure 2. Edge localized mode coil preliminary configuration

The following sections each address one of the four metals used in IVC construction to estimate the failure rate of each material in the ITER environment. Where possible, the operating experiences of these materials in radiation environments have been used to develop failure rates.

2. Oxygen-Free High Conductivity Copper Piping Failure Rate

Given that the ITER IVCs are inside the vacuum vessel and the ITER neutron flux is a significant factor in material lifetime, an effort has been made to determine copper tube failure rates in a nuclear environment. The IVCs need to withstand a 200°C bakeout temperature and a fast neutron fluence of up to 1E+23 n/cm^2 (Heitzenroeder et al. 2009).

The focus of this section is using oxygen-free high conductivity copper pipe for the resistive magnet conductor. The coil operates at 150°C, has a rating for 30,000 pulses, and is a 20-year lifetime component in the ITER vessel, positioned behind the blanket modules. From Figure 1, the copper pipe wall is 7.5 mm thick.

Tubing and piping are differentiated in that tubing is generally very low wall thickness (≤ 2 mm) and piping is more substantial wall thickness. The 7.5 mm wall thickness in this design is classified as piping. (For a malleable element like copper, the terms tubing and piping are sometimes used interchangeably but piping will be used in this section.)

2.1 Operating Experiences

A general source of copper conductor information is the toroidal field (TF) magnets of the Tokamak Fusion Test Reactor (TFTR). These resistive magnets operated for approximately 14 years on TFTR, culminating with deuterium-tritium plasma operations in the last 3 years of tokamak life. Therefore, the copper in these magnets has been exposed to at least some small level of high energy neutron fluence and perhaps some vibration as well. As always with operating experience failure rates, three values are needed: the operating time, the number of components, and the number of failed components. Each of these aspects is described below.

2.1.1 Operating Time

The TFTR operated from December 24, 1982, to April 4, 1997 (Machalek 1983; von Halle 1998). The typical approach used in data analysis for tokamaks at present is to count not just the "pulse seconds" of operation but to also count the preparation time, the ≈ 5-s pulse itself, and the post-pulse recovery time (diagnostic data archiving, machine cooldown, and machine configuration for the next pulse). This longer time is used because the tokamak systems are active and operating over that entire time interval (vacuum system, cooling systems, fueling systems are all "on," magnets and heating systems are at temperature, diagnostics operating, etc.).

The TFTR Group stated that in initial operation, the fastest time it could recover from a plasma pulse was 300 s (5 min) when removing magnet heat. After the TF magnet water coolant conversion to fluorinert in May 1993, the coil cooldown time was lengthened to 900 s (15 min) (Barnes et al. 1994; Barnes et al. 1995; Walton et al. 1994). Over its lifetime, TFTR produced more than 80,000 high-power plasmas (von Halle 1998). No data were found to properly partition the pulse counts in the deuterium-deuterium (D-D) and deuterium-tritium (D-T) operating periods, so a yearly average number of pulses was assumed. TFTR operated for 14.25 years, with an average of 80,000 pulses/14.25 yr = 5,600 pulses/yr. In the 1983 to early 1993 timeframe (10.33 yr), the operation time per pulse was 5 minutes. So the run time in that 10.33 years is estimated to be (5,600 pulses/yr × 10.33 yr × 5 min/pulse) giving 289,240 min or 4,820 hr of operating time. In late 1993 to 1997 (3.92 yr), the operation time per pulse was 15 min. Thus, the run time was 5,600 pulses/yr × 3.92 yr × 15 min/pulse, giving 329,280 min or 5,488 hr of operating time. These times are used rather than actual pulse durations because the tokamak systems are operating between pulses, the machine and systems are at operating temperature, with active cooling and power use, during the pulse day. The total hours would be 4,820 + 5,488 = 10,308 hr of operation. This would be a conservatively low estimate because the tokamak would not necessarily pulse as quickly as the magnets had cooled to a pulse-starting temperature. The pulse count estimate of

80,000 high-power pulses does not include the machine conditioning plasmas or the test plasmas where the magnets were used. Only the high-power plasmas are counted because these would have stressed the TF magnets more than the other types of pulses. The 10,308 hr of operation will be used for the TF coil operating time.

2.1.2 Number of Components

In this case, the length of copper in the TF magnets is sought. TFTR design data show that there were 20 TF coils in use on the tokamak (Smith and Punchard 1977) and there were 44 copper-copper joints within each coil. The conductor sections were about 35 ft long (Heitzenroeder 1991). Therefore, there were 35 ft × 44 joints = 1,540 linear ft (469.5 m) of copper conductor wound into one coil, and the copper conductor weighed 14 short tons or 12,700 kg/coil (Sabado and Little 1984).

The copper conductor was Copper Development Association 104 material specification (UNS C10400), an OFHC copper with 0.001% oxygen maximum and 0.027% silver as an alloying element. Figure 3 shows a sketch of the conductor, which came in three thicknesses (0.558, 0.607, and 0.683 in.) and one width, 6.547 in. The three thicknesses were used to help balance the temperature in the coil. Note in Figure 3 that the TF magnet conductor had a rectangular cross-section rather than a circular pipe cross-section as called for in the ITER IVC design. Despite this incongruity, the TFTR data are the best copper data set available due to the large amount of copper used, usage duration, failure reporting, and fusion environment. The design variation will be accounted for in the failure rate modifier values.

The TF magnet coils were initially held to a maximum operating temperature of 150°F (65.6°C) during pulse operations because of concerns about insulation integrity and material strength. The water coolant entered at 50°F (10°C) and each coil had a water flow of 150 gal/min (≈ 10 L/s) (Smith 1977). From Figure 3, the flow channel area is approximated as 0.270 in. × 0.803 in. = 0.21 in.^{2} or 1.398E−04 m^2. The flow velocity is the water volumetric flow rate divided by the flow area. Gettelfinger et al. (1989) stated that there were eight inlets and outlets per TF coil and that the volumetric flow rate to one coil was 10 L/s of deionized water. This flow rate translates to 0.01 m^3/s and, divided by eight flow paths, gives 0.00125 m^3/s in one flow path. Flow velocity = 0.00125 m^3/s ÷ 1.398E−04 m^2 or 8.95 m/s. This is a high velocity value but at the end of life when the conductor was under forensic inspection (Zatz 2003), the flow channels did not exhibit any notable erosion wear. When fluorinert coolant was used, the volumetric flow rate for the coil set was 160 L/s or 0.16 m^3/s (Walton 1994). For one of the twenty coils, the flow rate was 8 L/s or 0.008 m^3/s, and in one of the eight flow passages the flow velocity was 0.001 m^3/s. The flow velocity of that coolant in one coil was 0.001 m^3/s divided by 1.398E−04 m^2 or 7.2 m/s.

	A
PA	.558
PB	.607
PC	.683

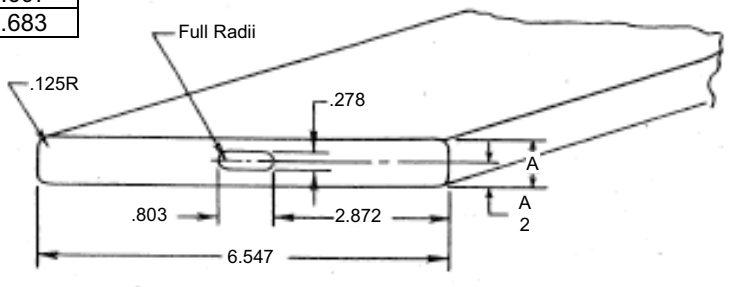

Figure 3. Sketch of the TFTR hollow copper conductor
Notes: This sketch was taken from Tobias (1979). Dimensions are given in inches; the coolant opening is 0.803 in. width × 0.270 in. height.

The joints in the conductor were made by induction brazing (Tobias 1979). The American Welding Society braze alloy BCuP-5, a 15% silver, 5% phosphorous, and 80% copper alloy, was used as the filler material. This brazing filler alloy is identified as UNS C55284. As mentioned by Heitzenroeder (1991), this filler is self-fluxing and no additional external flux was used in the braze. Water-cooled chill blocks were used during brazing to minimize the heat-affected zone of the braze. The joints were made carefully, with attention to detail and inspections of the work (Tobias 1979).

The TFTR conductor had three thicknesses as shown in Figure 3: the outer 4 turns were the thickest conductor, the inner 11 turns were the thinnest conductor, and the remaining 29 turns were the medium thickness conductor. For conservatism, the failure rate multiplier will be based on the highest wall thickness, which was (0.683 − 0.270)/2 = 0.2065 in. (5.25 mm) thickness. This thickness is conservatively chosen to mean less impact of the multiplier because the TFTR coils were not true pipes. The total length of copper conductor in 20 TF coils was 20 coils × 469.5 m/coil (9,390 m) of copper.

While in operation, TFTR generated D-D neutrons over the majority of its life and high-energy D-T neutrons in the latter years of its life. Kugel (1996) stated that the total D-T neutron yield was greater than 5.52E+20 neutrons. Reddan (1982) gave the circular torus dimensions as major radius R = 2.65 m and minor radius r = 1.1 m. The surface area of a circular torus is $4\pi^2 Rr$ so the TFTR torus surface area was $4\pi^2$(2.65 m)(1.1 m) or 115 m^2, which is 1.15E+06 cm^2. It is assumed that all the neutrons generated in the plasma will eventually penetrate the vacuum vessel wall.

The neutron energy is another issue. We assume that the neutrons at the magnets are still fast neutrons but are no longer 14 MeV—they have lost energy in collisions with graphite tiles, the stainless steel vessel, or the nitronic coil cases. Also, some neutrons leaving the vessel will not interact with the magnets—they will pass between the TF coils. The neutron fluence, to a first approximation, is ≈ 5.52E+20 fast neutrons/1.15E+06 cm^2 = 4.8E+14 n/cm^2. This fast neutron fluence is not a particularly high value; TFTR was meant to perform D-T experiments and not irradiate the materials to Greater Than Class C waste so that shallow land burial remained possible. Irradiation studies will be examined for insight to the proposed IVC operation.

2.1.3 Number of Failures

TFTR personnel documented several events with the TF magnets. Heitzenroeder (1991) mentioned that the TF coils had several instances of water leakage within the coils. At least two leaks were the result of cracks in oval copper tubing, which was additional coolant tubing brazed into the outer edge of a TF coil turn. That coolant tubing at the edge of the TF coils was extruded as a continuous length; it was not the TF conductor. There are insufficient data available on the tubing to include them in this assessment.

Zatz (2003) discussed coil examinations during the TFTR dismantling process for final disposal. One examination was of Coil #18, which had exhibited a chronic leak of the lead spur joint within the body of the coil. This spur joint for water coolant had a leak that defied all repair attempts during coil life. Coil #3 had developed several leaks in the fourteen water fittings at the base of the coil. The Coil #3 leaks were the motivation to change coolants from de-ionized water to fluorinert. Zatz stated that several TF coil bundles were cut from magnet Coils #3 and #18 for further investigation. When those TF coil bundles were being separated for metallurgical investigation, several turns had visibly detectable brazed joints where the lengths of copper conductor were spliced to form the wound coil. Every inspected joint had a flawless appearance and no evidence of wear or residual defect. Other, more cursory inspections of other coils also showed no concerns.

Inspection revealed that the copper in the immediate vicinity of the brazed joints was softer than typical conductor copper. This softer, lower strength copper region was attributed to high temperatures used during the brazing process locally annealing the copper. This effect had been anticipated in the coil design—the brazed joints were intentionally staggered by design to avoid a concentration of annealed copper in one location in the coil windings. The brazed joints were designed to be stronger than the local

copper, and all but one yield test specimen failed in the copper conductor rather than in the brazed joint. From this evidence, it would appear that none of the recorded leaks can be attributed to the TFTR TF copper conductors.

These findings raise the concern of accounting for the cooling water leaks from TFTR magnets. Zatz (2003) described the investigation of the water fittings on the sides of the TF coils. There were 14 fittings on each coil that routed water in and out of the coil, connecting to crosswise cooling channels machined into a conductor. Several of these water fittings were the cause of the water leaks that plagued the TF coils. There were two leaks in Coil #3 and one leak in Coil #18. Zatz investigated these water fittings and determined that the probable cause was that the crosswise channels (that is, side ports for water coolant entry and egress) were severely deformed and were not all centered in the thickness of the conductor turn, leaving a thin wall of copper. There were through cracks in the conductor turn. The reasoning in determining probable cause was that deformation during manufacturing and then brazing the water fitting to the copper plate led to locally annealed copper in the crosswise channel. When the conductor was wound into the coil turn, buckling could occur in the areas with thin walls. These leaks were not due to flaws in the copper conductor, they were the result of side channels machined in to the conductor and the braze heat from attaching fittings to those channels. Therefore, while there were three leaks in the life of the TF magnet coil set, to obtain a failure rate for the copper conductor without any side channels, the number of failures is taken to be zero because none of the TFTR conductor itself failed. If side channels are used in the ITER application, then several leaks must be used in the failure calculation.

2.1.4 Failure Rate Calculation

Assuming no failures in the copper conductor (based on the coil examination evidence), the average failure rate is calculated with the formula $\lambda = 0.5/T$, where T is the total operating time of the set of components (Atwood et al. 2003). Therefore, the average λ is 0.5/(9390 m × 10,308 hr) or 5.2E−09/m-hr. Since there were zero failures, no mode of failure was exhibited. Therefore, this failure rate would be applied to any failure mode, including small and large leakage, rupture, or blockage.

The upper and lower bounds are calculated by the Chi-square distribution. An upper bound failure rate (Atwood et al. 2003) with a 95% Chi-square distribution and 2n + 2 degrees of freedom (where n = number of failure events, $n = 0$) is $\chi^2(0.95,2)/2T$. The $\chi^2(0.95,2) = 5.99$ as found from Chi-square tables in O'Connor (1985). The upper bound failure rate calculation is 5.99/(2 × 9,390 m × 10,308 hr) or 3.1E−08/m-hr. The Chi-square 5% lower bound failure rate calculation for zero failures uses 2n + 1 degrees of freedom. The $\chi^2(0.05,1) = 0.103$ as found from Chi-square tables in O'Connor (1985). The 5% lower bound failure rate is 0.103/(2 × 9,390 m × 10,308 hr) or 5.3E−10/m-hr.

This "all modes" failure rate of 5.2E-09/m-hr from the TFTR TF magnet coils must be altered to apply to the ITER IVC coil. The factors of operating temperature, tube wall thickness, higher radiation exposure, flow velocity/flow media, and vibration must be considered. The TFTR TF coil data are summarized in Table 1. The ITER IVC coil parameters are given in Table 2.

Table 1. TFTR TF magnet coil parameters

Parameter	Value
Coil operating temperature	65.6°C with water 100°C with Fluorinert PF-5070
Conductor wall thickness	5.25 mm
Conductor radiation fluence	4.8E+14 fast neutrons/cm^2 (estimated value)
Flow media	Water for about ≈ 75% of lifetime Fluorinert PF-5070 for remaining lifetime
Flow velocity in one magnet channel	8.95 m/s for water 7.2 m/s for Fluorinert PF-5070

Table 2. ITER IVC magnet parameters

Parameter	Value
Coil operating temperature	150°C with water
Conductor wall thickness	7.5 mm
Conductor radiation fluence	3E+19 fast neutrons/cm^2 (estimated value)
Flow media	Water
Flow velocity in one magnet channel	3 m/s water for VS coils

2.2 Failure Rate Modifiers

The failure rate calculated from TFTR copper conductor will be modified to account for the ITER IVC parameters of operating temperature, tube wall thickness, flow velocity/flow media, radiation fluence, and vibration. The main parameters are summarized in Table 2 above. Each of these parameters is addressed below.

2.2.1 Operating Temperature

The TFTR coils operated for 10.3 yr of their 14.25-yr lifetime at a maximum operating temperature of 65.6°C. During the last years of service, when D-T operations were performed, the maximum temperature was 100°C. Because the 100°C (373 K) operation was during the highest stress of the magnet lifetime (full power shots and D-T irradiation), this operating temperature will be used here. Normally, an Arrhenius equation would be used for generating a failure rate modifier to account for a different operating temperature (Cadwallader 2010) but in this case, there are insufficient data available in the literature to determine the constants in the Arrhenius equation. After a wide literature search, there does not appear to be good data on copper piping in the open literature. Some qualitative data were found—Lewis (1999) and Cohen and Lyman (1972)—but these data were not supportive of a calculation for an operating temperature modifier because they were both at low temperature of potable water systems. Values at both low and high operating temperatures are needed to fit the equation. Perhaps organizations, such as the Copper Development Association, have data but those data are not openly available for use.

It is noted that the TFTR magnets had an initial service temperature ceiling of 65.6°C with concerns for insulation and structure. With the new coolant, the service temperature was increased to 100°C,

which is a full 34°C increase. This would indicate that the temperature increase was not a significant concern; the magnets operated for about one-third of their lifetime at this higher temperature. It is also noted that typical copper conductor in industry has ratings for elevated temperature operation, (ANSI 2011). For copper-to-copper connector joints, the test temperature is 100–105°C or 175–180°C above ambient temperature (ambient temperature is defined as 15–35°C). Given these allowable temperature ranges, it is apparent that copper can accommodate operation at 150°C without any significant impact to the failure rate. Joseph (1999) gave indication that brazed joints in copper piping systems routinely accommodate up to 177°C system operating temperatures without difficulty. Therefore, because copper piping can accommodate temperatures above 150°C in testing and in operations, the analyst judgment is that the temperature modifier should be equal to 1.0 to apply the TFTR failure rate to the IVC service temperature.

2.2.2 Wall Thickness

There are some qualitative observations on benefits obtained from increasing the tube wall thickness (Army 1977):

- Improved quality control of the tubing materials so pinhole leak possibilities are reduced
- Improved quality of tubing bends, giving less ovality and wrinkling
- Improved quality of attachments of end connectors (smaller heat affected zone)
- Easier handling before installation (small dents or scratches are not significant)
- Easier installation (the ends are more easily swaged, welded, or brazed)
- Less affected by the installed environment, more vibration resistant, more rugged.

Therefore, it is prudent to account for the tube or pipe wall thickness. In Cadwallader (2010), an expression based on the Thomas method was given when diameter and length are held constant:

$$\lambda_1/\lambda_2 = (t_2^2)/(t_1^2)$$

where

λ = failure rate

t = tube wall thickness.

Section 2.1.2 describes that the copper conductor is not a true pipe or tube so the larger form of this failure rate multiplier that accounts for the pipe diameter will not be used here.

If λ_1 = 5.2E−09/hr-m from the TFTR TF coils and t_1 = 5.25 mm, then for t_2 = 7.5 mm, the new failure rate can be found.

$$\lambda_1/\lambda_2 = (t_2^2)/(t_1^2)$$

$$\lambda_2 = \lambda_1/[(t_2^2)/(t_1^2)]$$

$$\lambda_2 = \frac{5.2E-09/hr-m}{(7.5\ mm)^2/(5.25\ mm^2)}$$

$$\lambda_2 = 2.55E-09/hr\text{-}m$$

Thus, the failure rate modifier for the increased wall thickness of the IVCs is

$$\frac{1}{\left[(7.5mm)^2/(5.25mm)^2\right]} = \frac{1}{2.04} = 0.49$$

2.2.3 Flow and Flow Media

In Table 1 the average flow velocity in a TFTR magnet cooling channel was given as 8.95 m/s for water, which is a high velocity value. In other tokamaks, the water velocity in magnet systems is limited from 1.5 to 1.8 m/s to minimize the effects of erosion (Gootgeld 1995). Copper ions in the effluent water have posed environmental concerns at DIII-D (Gootgeld 1993), so flow induced erosion-corrosion of the magnet cooling channel walls is an important issue to address not only for reliability but for environmental considerations as well.

There are several factors to consider in water cooling system flow velocities. The American Petroleum Institute (API) describes one issue of concern for carbon steel piping as general or localized corrosion of carbon steels and other metals caused by dissolved salts, gases, organic compounds, or microbiological activity. The API recommends that water flow velocities should be high enough to minimize fouling and "drop out" of deposits (i.e., precipitated solids from the coolant water) but not so high as to cause pipe wall erosion (API 2011). The API stated that low water flow velocities can promote increased corrosion. Water velocities below about 1 m/s are likely to result in fouling, sedimentation, and increased corrosion in systems using fresh water. Accelerated corrosion can also result from "dead spots" or stagnant areas if cooling water is used on the shell side of condensers/coolers rather than the preferred tube side. Pipe wall thinning tends to be uniform when flow velocities are low, but thinning will most likely be localized for high flow velocities associated with turbulent flow (API 2011). The magnets are assumed to be turbulent flow because of the high velocity, small cross-sectional area of flow, and the bends in the flow path.

Gagliardi (2000) stated that excessively high flow velocities of water in piping result in noise, vibration, and erosion. For water piping systems in general, a flow velocity range of 1.2 to 4.5 m/s is acceptable. The velocity value in this range depends on the pipe material, the system design, and the pipe size. Brass pipe can be 1.2 to 4.5 m/s but carbon steel pipe should be in the 2 to 3 m/s range. Water velocities up to 9.1 m/s could be acceptable if the material is less susceptible to erosion, such as stainless steel. Reducing vibration while meeting the system's hydraulic requirements reduces susceptibility to flow-induced erosion. These velocity ranges are only recommended if the system operational requirements are also satisfied. However, high velocities are also conducive to water hammer problems in the cooling system.

The Copper Tube Handbook (Copper Development Association 2010) gives water velocity limitations to avoid excessive noise and erosion-corrosion. Cold water systems should not exceed 8 ft/s (2.4 m/s) and hot water systems (up to 140°F or 60°C) should not exceed 5 ft/s (1.5 m/s). In systems operating hotter than 60°C, the water velocity should be in the range of 2 to 3 ft/s (0.6 to 0.9 m/s). It should be noted that this guidance is for copper tubing systems where the copper is thin-walled tubing. The handbook also notes that copper tubing normally retains a smooth bore throughout its service life and does not require design allowances for corrosion, scaling, and caking from the coolant impurities.

The flow media for the TFTR coils and the IVC coils is the same: water. The water used for cooling resistive magnets is meant to be very clean. The water is deionized, de-oxygenated, and impurities removed. Calcium and magnesium impurities (the principal elements in scale deposits) are removed as well as sulfates, chlorides, carbonates, and silica. The cooling water is also typically filtered with 150-micron wire mesh strainers and 75-micron filters, and some water is also circulated through 5-micron filters (Gootgeld 1995). Because water is uniformly used for the TFTR and ITER applications, the failure rate modifier is 1.0 for the coolant type. Another concern with water coolant is microbial contamination,

as mentioned above. Without any information, and the knowledge that copper is sometimes used to reduce biological fouling, a factor of 1.0 will be assigned to microbial issues.

To set bounds on the failure rate multiplier, operating experience was examined. The two most well-known cases of flow induced erosion-corrosion led to wall thinning of the feedwater piping in the Surry 2 and Trojan power plants in the U.S. (Smith 2001). Using a piping failure rate from the *Reactor Safety Study* (U.S. Nuclear Regulatory Commission [NRC] 1975) that was prevalent at the time gives a piping rupture failure rate of 1E−10/hr-section. A pipe section is historically taken to be 10 to 100 ft length; in this case, a section is assumed to be 10 ft of pipe run between welds or valves, etc. Thus, the average failure rate is taken to be 1E−09/hr-ft. The main feedwater piping in a power plant is taken to be 5,900 ft as given by Wright et al. (1987); half of that (2,950 ft) is assumed to be large diameter piping.

The Surry 2 plant began operation in 1973 and the failure occurred on December 9, 1986 (about 14 yr after beginning operation) at an assumed 75% per year of power operation. Thus, 14 yr × 8,760 hr/yr × 0.75 = 91,980 hr. The main feedwater piping rupture probability for Surry 2 in 1986 would have been 1E−09/hr-ft × 91,980 hr × 2,950 ft or 0.27. Because the piping wall thinned prematurely, the rupture failure was due to insufficient piping wall strength. The multiplier on the failure rate would have been 3.7 to account for the one flow-accelerated corrosion (also called erosion-corrosion) failure event.

The Trojan plant, which began operation in 1976, had its feedwater piping failure in March 1985. Using 9.25 years of operation gives 9.25 yr × 8,760 hr/yr × 0.75 = 60,773 hr. The same 2,950 ft of piping is assumed, giving 1E-09/hr-ft × 60,773 hr × 2,950 ft or 0.18. The multiplier on the piping failure rate would be 5.6 to account for the flow-accelerated corrosion.

From this exercise, we see that the failure rate multipliers are in the range of 3 to 6 for carbon steel piping, which is reputed to be susceptible to flow accelerated corrosion in power plants. Perhaps copper piping is not as susceptible as carbon steel, but little data were found in the literature on the behavior of copper. An assumption is made that copper, a more malleable material than steel, will behave no worse and no better than the carbon steel. A factor of 6 is taken as the overall highest multiplier for flow accelerated corrosion.

Using the work by Chexal et al. (1998), we estimate that flow accelerated corrosion is increased by a number of multiplicative factors:

- Temperature of the flow system
- Wall alloy content
- Mass transfer effect of protective oxide coating parting from the wall to the fluid
- Oxygen in the water effect
- pH of the water effect
- Geometry effect that promotes turbulence
- Void fraction in the water effect
- Hydrazine concentration in the water effect.

Each of these eight effects will be given an engineering judgment value based on IVC system information. Because the preliminary calculation based on the power plant experience showed variation between 3 and 6 as the overall failure rate modifier, and because no single corrosion effect listed above is stated by Chexal to be more important than other effects, analyst judgment is used to set the failure rate modifier values for any one effect to a maximum of $(6)^{1/8} = 1.25$. Each judgment on a modifier value is described below.

Temperature Effect. For carbon steel, temperatures between 110 and 150°C make pipe highly susceptible to flow accelerated corrosion (Vanderhoff et al. 2012). The water solubility of the oxide layer that protects the pipe wall from additional oxidation varies with water temperature. For copper, oxide forms to protect the pipe wall surface (Liptakova et al. 2010). The solubility peaks of cupric and cuprous oxides in water are at a higher level, more in the 150 to 350°C range with a high value at 250°C (Palmer and Benezeth 2004). Recalling that the maximum multiplier would be 1.25 for this effect, then ratioing a 1.25 − 1.0 = 0.25 multiplier change with the ΔT of 100°C gives 0.0025/°C in the range given by Palmer. The failure rate modifier for the IVCs will be assigned as 1.0025 because the IVC operating temperature is just at the low end of the peak solubility temperature range for copper oxides.

Wall Alloy Effect. This factor was developed by Chexal et al. (1998) to take into account the elements of chromium, copper, and molybdenum in steel. Chromium as low as 0.1% in the metal has been shown to significantly reduce flow accelerated corrosion in carbon steel (Vanderhoff et al. 2012). The copper effect is not as pronounced as that of chromium. This factor for the IVCs will be assigned as 1.0 for wall alloy because this is judged to not have an effect for all-copper piping.

Mass Transfer Effect. This effect accounts for flow velocity, pipe diameter, coolant turbulence, and other hydrodynamic factors. This effect tends to be the most recognized because it incorporates the flow velocity. The IVC coils will have ≈ 3 m/s flow in the copper vertical stabilizing coils. This is a higher flow velocity than other resistive magnet coils, such as the DIII-D coils that had 0.5 m/s in the ohmic heating coil and 1.6 m/s flow in the field shaping coils (General Atomics 1989). These flow velocities are lower than the 8.95 m/s water velocity used in the TFTR TF coils. Chexal et al. (1998) stated that the mass transfer effect $k = (Sh)(D)/(d_H)$, where Sh is the Sherwood number, D is the diffusion coefficient for the pipe wall material in the coolant, and d_H is the hydraulic diameter of the pipe. Ratioing the k numbers (k_{IVC}/k_{TFTR}) for the ITER IVC and TFTR conditions will give the failure rate modifier to the TFTR copper magnet to apply to the IVC.

When the mass transfer k values are ratioed, the D values are close to each other because both applications are copper with water coolant and only a small temperature difference. Therefore, the D values are assumed to cancel each other. The hydraulic diameter for the TFTR coolant passage is $d_H = 4A/P$ where A is the cross sectional area and P is the wetted perimeter. From Figure 3 and the discussion above, for TFTR coils the flow area A = 1.398E−04 m^2 and P = 2.16 in. or 0.055 m. Then the TFTR d_H = 0.0102 m. For the hydraulic diameter of the IVC coil, d_H = diameter of the circular channel, or 0.03 m (see Figure 3). The Sherwood number is a function of the Reynolds number and the Schmidt number, but Chexal does not define the relationship. Turning to the Perry's handbook (Green and Maloney 1997), for tubes in turbulent flow, the Sherwood number $Sh = 0.023(Re)^{0.83}(Sc)^{0.33}$. The Reynolds number, Re, is equal to vL/ν where v = fluid velocity, L = tube length, and ν = kinematic viscosity of the fluid. The Schmidt number $Sc = \nu/D$ where ν = kinematic viscosity of the fluid and D = mass diffusivity. The ratio will be

$$k_{IVC}/k_{TFTR} = \frac{[(0.023(\mathrm{Re})^{0.83}(Sc)^{0.33}(D)/(d_H)]_{IVC}}{[(0.023(\mathrm{Re})^{0.83}(Sc)^{0.33}(D)/(d_H)]_{TFTR}}$$

Cancelling out like terms in the numerator and denominator leaves

$$k_{IVC}/k_{TFTR} = \frac{[(v)^{0.83}/(d_H)]_{IVC}}{[(v)^{0.83}/(d_H)]_{TFTR}}$$

$$k_{IVC}/k_{TFTR} = \frac{[(3m/s)^{0.83}/(0.03)]_{IVC}}{[(8.95m/s)^{0.83}/(0.0102m)]_{TFTR}}$$

$$k_{IVC}/k_{TFTR} = 0.137$$

The TFTR copper failure rate should be reduced to account for the ITER IVC mass transfer conditions. This modifier should be 0.137 to account for the mass transfer effects of flow accelerated corrosion for the IVC coils.

Oxygen Effect. Flow-accelerated corrosion varies inversely with the amount of dissolved oxygen present in the water. Vanderhoff et al. (2012) stated that some dissolved oxygen is needed in the fluid to promote formation of a protective oxide layer. The experience for carbon steel piping shows that keeping the dissolved oxygen between 50 and 100 ppb will significantly minimize or prevent flow-accelerated corrosion. However, that amount of dissolved oxygen can promote corrosion in heat exchanger components not constructed of carbon steel, so a compromise of > 1 ppb oxygen to reduce pipe wall corrosion and < 50 ppb oxygen to prevent heat exchanger tube corrosion is used. The IVC water coolant will be deionized and deoxygenated. Dortwegt and Maughan (2001) discussed that for water cooling of copper tubing, the dissolved oxygen in water would peak at 200–300 ppb, so operating at less than 50 ppb is advisable, close to 1 ppb oxygen is optimum. An assumption is made that the designers will specify to control oxygen concentration in the cooling water so that an optimum, or close to optimum, level will be present to maintain the protective oxide while accounting for radiolytic decomposition of water molecules to keep the dissolved oxygen to low values that do not corrode the flow loop materials. The oxygen factor will be assigned a value of 1.0.

pH Effect. Chexal et al. (1998) discussed that the rate of metal loss from the wall depends on solubility of the metal ions at the metal surface. In general, for carbon steel, a pH closer to 8 will give a high corrosion rate and a pH closer to 9.5 will give a much lower corrosion rate, about 6 times less than the value at pH of 8. Thus, assuming that the pH of the cooling water for the ITER IVCs is kept to an optimum value for copper, then the pH factor will be given a value of 1.0.

Geometry Effect. In the carbon steel piping, this issue is generally concerning bends, elbows, control valves, and orifices in the flow stream that cause the water to impact or sweep over pipe surfaces downstream of these features. Corrosion is increased wherever the water is forced to turbulently sweep a pipe surface. The IVCs will have high turbulence and several bends per IVC turn. Therefore, a maximum factor of 1.25 is assigned to account for the geometry effect.

Void Fraction Effect. Steam voids in the water can collapse and damage the pipe walls. The cooling water in the IVCs is pressurized and is expected to remain subcooled and have zero voids, even around bends in the IVCs. The factor for the IVCs will be assigned as 1.0 for the void fraction effect.

Hydrazine Concentration Effect. The cooling water in the IVCs is not anticipated to require large addition of a reducing agent such as hydrazine. Chexal et al. (1998) gave some performance curves for various concentrations of hydrazine from 0 to 150 ppb. For 150°C operation, at 0 and 20 ppb hydrazine in water, the corrosion rate increases from 0.018 in./yr of wall thickness to 0.034 in./yr of wall thickness. The 20 ppb will be assumed here as the hydrazine needed in the IVCs. At 150 ppb hydrazine, the corrosion rate reaches 0.08 in./yr of wall thickness. Ratioing these corrosion rates gives

$$(0.034 - 0.018)/(0.08 - 0.018) = (x - 1)/(1.25 - 1)$$
$$x = 0.065$$

so the multiplier would be 1 + 0.065 or 1.065 to account for 20 ppb hydrazine.

The overall flow and flow media value is the product of coolant factor (= 1.0 because both applications use water) and eight flow corrosion factors or
$(1 \times 1.0025 \times 1 \times 0.137 \times 1 \times 1 \times 1.25 \times 1 \times 1.065) = 0.183$.

It should be noted that in 1997, the FermiLab main injector experienced numerous pin-hole size, thru-wall leaks in the stainless steel piping of the main injector's magnet water cooling system (Hurh 1999). Most of the piping is 6-in. diameter, Schedule 10 wall thickness, 304L stainless steel. A new stainless

steel header system had been installed a few months before for each of the six cooling subsystems, and it had passed its hydrostatic pressure testing. The system had been granted permission to begin operations. Chlorinated well water was used for the pressure tests. The system volume is 66,000 gal, so water from one subsystem test was reused by sending the volume to another subsystem and filling with more well water when needed. The pressure tests of all six subsystems were completed over a 6-month period. When the circulation pumps were started, some leaks were found in weld joints. A few leaks were found more than 1 in. away from pipe welds. Over a few days, the number of pinhole leaks grew to approximately 400. The water was sampled and high levels of aerobic/low nutrient bacteria and traces of sulfate-reducing bacteria and iron-related bacteria were found. The effects of these bacteria were termed microbiologically influenced corrosion (MIC (bacteria layers form and preclude oxygen from contacting the metal surface to maintain the passive oxide layer on the pipe's metal surface). The staff added ammonium and glutaraldehyde to the water to control the bacteria growth, then the pipework was drained and dried. Welds were inspected by either radiographic inspection or visual inspection with a remote robotic camera. Of the 10% of the accessible welds that were radiographed (208 welds out of 5400 welds in the system), 61% of those 208 welds showed flaws from MIC. This type of failure is not accounted for in the failure rate modifier. It is believed that the designers will note the high level of downtime associated with weld repairs at FermiLab and take steps to preclude high levels of bacteria in the cooling water system for the IVCs. Gootgeld (1995) noted that bacteria contamination also exists in the DIII-D cooling water. At DIII-D, colony-forming organism concentrations or "colony-forming units" (cfu) range from 30 to 130 cfu/mL and total oxidizable carbon ranges from 2.5 to 5 ppm. Biocide control, such as ultraviolet radiation or chemical addition to the water, has not been recommended as necessary by consultants for DIII-D cooling water. DIII-D has not observed deleterious effects from bacteria in cooling water at up to 130 cfu/mL.

2.2.4 Radiation Environment

Zinkle and Busby (2009) discussed the radiation damage processes that occur in structural materials at different temperatures and fluence levels. Radiation hardening and embrittlement are generally the low temperature phenomena of concern (that is, at less than 0.3 to $0.4T_{melt}$ when T_{melt} is in Kelvin) when neutron damage is > 0.1 displacements per atom (dpa). Other phenomena emerge at higher temperatures and dpa levels. Because the melting temperature of copper is about 1,353 K (1,080°C) and the operating temperature is 423 K (150°C), then 423 K/1,353 K = 0.313, which is within the lower end of the suggested temperature band for radiation hardening and embrittlement of the copper conductor. Therefore, factors to account for hardening and embrittlement will be used to modify the failure rate from the TFTR coils to apply to the ITER IVCs.

TFTR generated D-T neutrons in the latter years of its life. The neutron fluence, to a first approximation, was estimated to be 4.8E+14 n/cm^2. This fast neutron fluence is not a particularly high value. The TFTR magnets did not give any indication of material radiation damage; there was no mention of swelling or brittleness in the post-service examination (Zatz 2003). Despite the coolant leaks mentioned earlier, the magnets performed well to the end of service. Copper irradiation studies will be will be needed to adjust the copper failure rate for high neutron fluence.

Heitzenroeder et al. (2009) gave an initial estimate of the neutron fluence as 1E+23 n/cm^2 for the IVCs. More recently, neutronics calculations for the VS and ELM coils give peak values of fast neutron flux (Sawan 2012). For the lower VS coil, the fast neutron flux is 2.17E+13 n/cm^2-s and is multiplied by 1.66E+07 s for a cumulative fluence of 0.3 MW-yr/m^2, which gives a fast neutron fluence of 3.6E+20 n/cm^2. For the upper VS coil, the fast neutron flux is 1.27E+13 n/cm^2-s or a fluence of 2.1E+20 n/cm^2. Thus, the greatest fluence of fast neutrons is 3.6E+20 n/cm^2.

The radiation damage will affect two important properties of the IVCs; the strength and the electrical resistivity. The magnets need to maintain structural strength and not become brittle to function properly. If radiation damage increases the electrical resistivity then the magnets cannot operate at rated conditions

over their service lifetime. These two properties will be addressed separately. The radiation damage failure rate modifiers will follow the approach used by Lauridsen et al. (1996). The radiation degradation factor is

$$\Delta = [P_o - P_t]/[P_o - P_f]$$

where

P_o = value of a characteristic parameter of the material before radiation exposure

P_t = value of a characteristic parameter of the material after total radiation dose

P_f = value of the characteristic parameter of the material at failure.

This Δ degradation factor varies between 0 and 1, showing the parameter margin remaining in the material under irradiation. This factor assumes that any radiation effect depends on the dose level to see the change in the characteristic parameter. When Δ approaches 1, P_t is approaching P_f, so the material is radiation degraded. As Δ approaches 0, the material in question has seen low dose and is not degraded.

The Δ degradation factor must be translated into a failure rate modifier. While a lower bound for a radiation damage modifier is assumed to be 1.0, other materials have been examined to help set the upper bound for the modifier. It is granted that electronics are more sensitive to radiation than metals, but electronics give some indication of the effects of radiation because they have been tested for service life after irradiation. Often a threshold dose is given for the onset of degradation and the same is true for metals (Ma 1983). Bajenescu and Bazu (1999) discussed semiconductors, where the gates can withstand 100 k-rads over their service life with no process changes. A radiation-hardened gate can withstand 1 Mega-rad over the same service life with no process changes. Thus, a factor of 10 is seen for the failure rate of semiconductors, which can translate to longer semiconductor lifetime at low irradiation or adequate service life at high irradiation. Comparisons of irradiated and unirradiated flash memories show factors of 2 to 4.5 overall performance degradation with irradiation (Oldham et al. 2009; Oldham et al. 2011). Fiber optics showed 20 times the attenuation of light when irradiated (Gill et al. 1997). This small sample of electronics items shows factors of 2 to 20. Other radiation *k* factors for other equipment are given in Table 3 below. These span a range of 1 to 5.

The effects of radiation vary, with *k* factors of 1 to 20. It is noted that a factor of 10 has been used as the difference between the failure rates of a low mechanical stress and high mechanical stress metal part (shafts, bolts, etc.) (Green and Bourne 1972). Because radiation damage can change the stress response of metals, this factor of 10 was noted as significant. Given the spread of radiation damage multipliers, especially the low multipliers in Table 3 for low neutron fluence, an assumption is made that a failure rate modifier of 10 will be used to demonstrate a significant degradation. In this case, the degradation is a strength change due to irradiation. The factor of 10 will be applied to each mechanical property identified as an issue for radiation damage; this should result in a conservative estimate of the overall radiation damage to the copper given what is known of failure rate modifiers described above. However, it is recognized that this is analyst judgment—no high fluence operating experiences with copper were found in a literature search. For the radiation damage failure rate modifier, to account for the factor of 10, the Lauridsen radiation degradation factor is used as

$$\textit{Failure rate modifier for radiation damage} = 10^{(\Delta)}$$

In that way, when the material is unaffected by radiation and Δ is 0, then $10^0 = 1$, giving the failure rate modifier of unity. As Δ tends to one, meaning high radiation degradation of the material property, then the modifier value approaches 10, which is the assumed value for increasing the failure rate of a metal in a high fluence neutron radiation field.

Table 3. Some failure rate modifiers for radiation environments (IEEE 1984)

Component Type	K factor Failure Rate Multiplier
Annunciators	1.1 to 2.0
Batteries	1.05 to 1.2
Blowers	1.0
Circuit breakers	1.17 to 5.0
Motors	1.0
Heaters	1.0
Transformers	1.07 to 1.57
Valve actuators	1.1 to 2.06
Instrumentation & Controls	1.0 to 1.25
Cables	2.0 to 3.7
Note: The radiation environment is that found in the interior of a containment building of a nuclear fission power plant. This environment includes both MeV gamma and 10–100 keV neutron fluxes. The combined radiation field is on the order of 0.1 to 0.25 Sv/hr, where ≈ 10% is due to neutrons and the remainder is gamma radiation (Prince 2012). This dose rate range is converted to fluence by conversion factors given by Tsoulfanidis (1983) and assuming a 20-yr component lifetime. The neutron fluence ranges are 1E+13 to 1E+14 n/cm^2 and the gamma fluence ranges are 1E+15 to 1E+19 γ/cm^2. The neutron flux is in fair agreement with measurements made by Scherpelz and Tanner (2002).	

The properties of copper before and after irradiation are taken from radiation damage studies. Vendermeulen (1986) gave data points for cold worked and annealed copper before and after irradiation. The yield strength before 5 dpa irradiation is 225 N/mm^2 (225 MPa), so the initial parameter P_o = 225 MPa. Vandermeulen tested copper at 150°C irradiation temperature and gives a post-irradiation yield stress of 190 MPa. The parameter after irradiation is P_t = 190 MPa. The parameter at component failure (P_f) is assumed to occur at stress and = 2/3 × yield strength based on metals in the ASME Boiler and Pressure Vessel Code. In this case, that value is 150 MPa.

With these data, Δ can be calculated:

$$\Delta = [P_o - P_t]/[P_o - P_f]$$
$$\Delta = [225\ MPa - 190\ MPa]/[225\ MPa - 150\ MPa]$$
$$\Delta = 0.47$$

and

Failure rate modifier for radiation damage $= 10^{(\Delta)}$
Failure rate modifier for yield strength radiation damage $= 10^{(0.47)}$
Failure rate modifier for yield strength radiation damage = 2.95

Vandermeulen (1986) also gave plots for elongation of copper samples, which accounts for embrittlement. Unirradiated copper was 42% elongation (P_o = 0.42), and at 150°C irradiation temperature the irradiated copper was about 38% (P_t = 0.38). To set the elongation at failure, a conservative approach was used. While copper is a malleable material, there is a concern for copper to become brittle. Juvinall and Marshek (1991) suggested that a safety factor of 2 or even 3 be used with brittle material. Juvinall and Marshek stated that if elongation drops below 10%, the design should be

examined for using a less brittle material. So, a failure is assumed when elongation reduces to a value of 3 × 10% elongation or $P_f = 0.3$. In that case, Δ is

$$\Delta = [P_o - P_t]/[P_o - P_f]$$
$$\Delta = [0.42 - 0.38]/[0.42 - 0.30]$$
$$\Delta = 0.333$$

and

Failure rate modifier for radiation damage $= 10^{(\Delta)}$
Failure rate modifier for elongation radiation damage $= 10^{(0.333)}$
Failure rate modifier for elongation radiation damage = 2.15

Brager (1986) showed electrical conductivity values for fast neutron irradiated copper alloys, and the conductivity did not begin to decline until the neutron fluence reached 1E+22 n/cm^2. Brager stated that creation of nickel and zinc activation products in the copper matrix was a large factor in the electrical conductivity decrease. Fabritsiev and Pokrovsky (1997) also showed that electrical resistivity of copper only began to decline in the 1E+21 n/cm^2 and greater fluence range. Zinkle (1992) stated that ≈ 0.1 dpa is about 1E+20 n/cm^2 fluence for copper. This gives radiation hardening, which is believed to increase the electrical resistivity. Eldrup and Singh (1998) stated that for 0.1 dpa neutron fluence, the electrical conductivity of copper was at 91% of the unirradiated value. Less fluence would result in higher conductivity. At 3.6E+20 n/cm^2 fluence, the electrical conductivity decrease is not expected to be very large so the failure rate multiplier is assumed to be 1.0 for radiation effects on electrical conductivity for the expected IVC fluence.

The radiation damage multiplier accounts for copper strength change, copper embrittlement, and electrical resistivity and is 2.95 × 2.15 × 1.0 = 6.34.

2.2.5 Vibration Environment

The TFTR magnets were in a fusion environment but they were not inside the vacuum vessel so, while these magnets probably experienced some vibration, it was likely much less than that of in-vessel components. For example, the JT-60 reactor had large vibrations from plasma disruptions (Kishimoto et al. 1998). The JT-60 vacuum vessel would experience up to 41.4 gravities horizontal and 38.5 gravities vertical acceleration at a 50 Hz frequency over 30 ms from membrane vibrations caused by disruption forces. The amplitude of the vacuum vessel motion was not given. Wowk (1991) gives an equation to determine the amplitude of a vibration, $D = 9.78g/Hz^2$. For $g \approx 40$ and 50 Hz, $D = 0.156$ in. or about 4 mm. The JT-60 vibrations caused some air leaks in flanges and valves attached to the ports on the vessel sectors. There was no discussion of magnet damage from vibration at JT-60; the discussion focused on the vessel and the ports attached to the vessel.

The TFTR magnet coil turns were epoxied together to form cohesive units and they were encased, so there was little turn-to-turn vibration expected. Published TFTR operating experiences did not discuss magnet vibrations, so it is assumed that the TFTR magnet vibrations were low—they did not create fatigue in the copper conductor.

A military standard (U.S. Department of Defense 2002) discusses testing electrical components of weight under 136 kg (300 lb), such as transformers, relays, switches, and other components that use electrical copper. The vibration test includes three frequency ranges (10–500 Hz, 10–2,000 Hz, and 10–3,000 Hz), and tests between 10 and 80 gravities peak acceleration. It is noted that the vibration frequency for the IVC coils is expected to be 5 Hz (Daly et al. 2012), which is below the frequency range for military equipment testing.

As seen from the frequency ranges given above, there are some low frequency vibrations in mechanical equipment that do not pose degradations to the equipment itself or to proximate equipment. Wowk (1991) gave an example of a centrifugal pump turning at 1800 revolutions per minute; this is a 30-Hz vibration. Wowk also gave a range of allowable vibration parameters that do not detract from machine lifetime. These are 0.003 to 0.1 gravities peak, 20 to 600 Hz, and less than 0.005 mm displacement. However, flow-induced vibration of small diameter piping (diameter of 50 mm and less) is known to be a vibration fatigue cracking concern for fission power plant piping (Bush et al. 1996; Fleming and Lydell 2006).

FIDES (2010) gives a relation for a failure rate modifier to account for vibration. This formula is called Basquin's Law and is said to apply to aluminum, copper, glass, ceramics, and other materials:

$$AF = (g_{rms}/g_{rms0})^{1.5}$$

where

AF = the failure rate modifier for acceleration factors

g_{rms} = the root mean square vibration amplitude (measured in gravities) in the operating environment

g_{rms0} = a reference vibration amplitude

The FIDES recommended 0.5 g_{rms} for the materials listed above.

A report on failure rate modifiers (National Aeronautics and Space Administration [NASA] 1971) gives vibration *k* factor data on some electrical equipment that uses copper connectors and switches. For ambient conditions, the *k* factor is 1.0. Ambient conditions are considered to be zero vibration. The connector data showed *k* factor variation from 18 to 86 for acceleration of 10 to 50 gravities—root mean square (g_{rms}). To convert the root mean square gravities to peak gravities, multiply by 1.414. The electrical switch data showed *k* factor variations of 60 to 180 for an acceleration of 10 to 40 g_{rms}. These data are linear for the two components and also for most of the other components in the cited report. It is noted that vibration *k* factors tend to be up to 30× larger than other types of *k* factors, especially when the acceleration is high.

The IVC coil frequency is expected to be 5 Hz and the gravities are expected to be much less than the 40 gravities discussed for the JT-60 disruptions (the ITER vessel is double-walled and heavier than the JT-60 vessel and it has more supports). The ITER load cases for the vacuum vessel give pressures on the vessel for disruptions and give the seismic event accelerations. An ITER seismic level 2 (SL-2) event gives vacuum vessel radial acceleration of 4.6 m/s^2 (0.47 gravities) at the supports, toroidal acceleration of 1.47 m/s^2 (0.15 gravities) at the bottom of the vessel, and vertical acceleration of 27.8 m/s^2 (2.8 gravities) at the inboard vessel wall (Martinez 2012). Operational vibrations must be less than rare SL-2 earthquakes, which are severe events. A value of 1 gravity peak acceleration at 5 Hz would be 10 mm amplitude, more than expected, but a 1 gravity peak or 0.707 g_{rms}, is assumed for the IVC coils in typical operation. With this assumption, $AF = (0.707/0.5)^{1.5}$ gives a failure rate modifier of 1.68.

2.3 Final Failure Rate Value

The TFTR copper magnet piping failure rate value was calculated as 5.2E−09/m-hr for all failure modes. That is, this failure rate would be applied to any failure mode, including small and large leakage, rupture, or blockage. The Chi-square 95% upper bound failure rate is 3.1E−08/m-hr. The Chi-square 5% lower bound failure rate is 5.3E−10/m-hr. The failure rate multipliers to apply to the TFTR copper failure rate for application to ITER IVCs are given in Table 4 below. The overall failure rate multiplier is 0.954.

Thus, the "all modes" copper piping failure rate to apply to the ITER IVC conductor is (0.954 × 5.2E−09/m-hr) or 4.96E−09/m-hr. This value is rounded up to 5E−09/m-hr. The upper and lower bounds are 3E−08/m-hr and 5.1E−10/m-hr, respectively.

Table 4. Copper piping failure rates and adjustment factors

Calculated Failure Rate and Failure Mode (/hr-m)	Operating Temperature Factor	Wall Thickness Factor	Flow and Flow Media Factor	Radiation Factor	Vibration Factor	Resulting Value for IVC Use (/hr-m)
Mean 5.2E−09 all modes	1.0	0.49	0.183	6.34	1.68	4.96E−09 or ≈ 5E−09
95% bound 3.1E−08 all modes	1.0	0.49	0.183	6.34	1.68	3E−08
5% bound 5.3E−10 all modes	1.0	0.49	0.183	6.34	1.68	5.1E−10

3. Stainless Steel Tubing Failure Rate

The ITER IVCs for plasma VS control will use a stainless steel jacket around the magnesium oxide insulation. Given that these water-cooled coils are inside the vacuum vessel and the ITER neutron flux is a significant factor in material lifetime, an effort has been made to determine stainless steel failure rates in a nuclear environment. The IVCs need to withstand a 200°C bakeout temperature and initially the fast neutron fluence was thought to be on the order of 1E+23 n/cm^2 (Heitzenroeder et al. 2009). The preliminary VS coil configuration is shown in Figure 1.

The focus of this chapter is the stainless steel 316 jacket of the coil since there is a concern of release of foreign materials (the particulate MgO insulation if there is a major failure) or possibly coolant water into the vacuum vessel (Heitzenroeder et al. 2009). The largest use of stainless steel tubing in a high radiation environment has been the fission fuel element cladding of fast neutron reactors. While fission neutrons are born typically at ≈ 2 MeV rather than 14 MeV for D-T neutrons, the fission data have been shown to provide similar displacement damage to fusion neutrons (Zinkle et al. 2002) and fission irradiation remains the closest large body of experience data available to apply to the IVCs.

The basic failure rate calculation is the number of failures in the set of components divided by the product of the total number of components and the time period of operation. That is

λ = *failure count/(component count × operating time)*

Often, the number of failures is readily available from failure reports, but the denominator information usually requires more effort to obtain from operating experiences.

3.1 Operating Experiences

The Experimental Breeder Reactor-II (EBR-II) operated at power from 1964 to 1994 at the Idaho National Laboratory. This reactor initially used stainless steel 304L fuel element cladding. The fuel cladding tubes were 0.3 mm thick (Seidel and Einziger 1977) and were about 441 mm in length (Stevenson 1987). A fuel element is shown in Figure 4. This fission reactor used a small core with a high fast neutron flux of 1E+15 n/cm^2-s (Koch 1988). One fuel assembly comprised 91 tubes. There were 53 fuel assemblies used in one core loading plus 12 control rod assemblies that each had 61 fuel tubes in one core loading (Koch 1988). The cladding for fuel assemblies and control rod assemblies were identical in alloy and dimensions. The reactor used seven cores from 1965 to 1969 (Stevenson 1987) and typically one core per year after 1969. The technology for fabricating the fuel assemblies in the hot cell matured, and after completing tests to high fuel burnup (greater than 10 atom%) to intentionally fail cladding (Seidel and Einziger 1977), the plant operated with less than one tube breach failure per core (Walters 1999). The breaches experienced in operations were typically intergranular cracks, often at the restrainer "dimples." These dimples were indentations to prevent the metallic fuel bar inside the cladding tube from ratcheting upward in the tube then dropping back down to the bottom of the tube—thereby creating a neutron reactivity insertion event in the core during reactor operation (Walters 1999). The failure mode of these tubes was predominantly breach by cracking. This experience gives a failure mode of breach and < 1 tube breach per core.

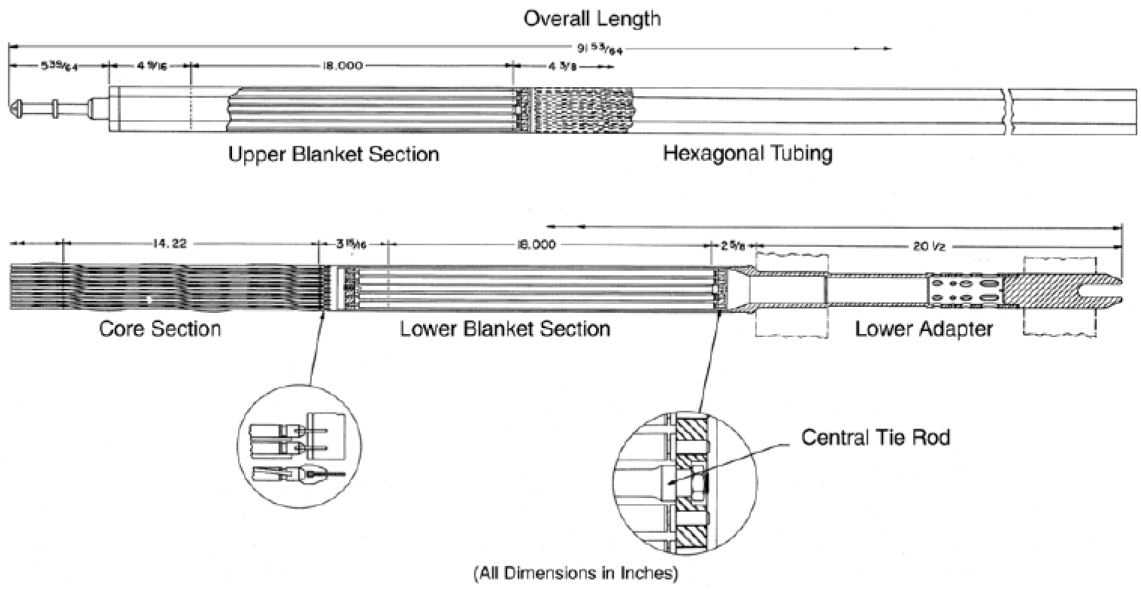

Figure 4. An EBR-II fuel assembly (Koch 1988)

3.1.1 Failure Rate Calculation

The EBR-II plant was intended to generate electricity as well as demonstrate a closed fission fuel cycle. The plant capacity factor is defined as

[MWth-hours produced/(calendar-hours × 62.5 MWth)] × 100%

The plant rarely, if ever, operated at partial power because it was expected to generate 20 MWe. This means that the capacity factor was basically hours at power/calendar hours for any given year, which is the same as plant availability. Some capacity factor data are given in Table 5.

EBR-II had an average availability of 59.8% (see Table 5), so 8,760 hr × 0.598 ≈ 5,238 hr average core operation in a given year before core changeout. We can conservatively say

$$\lambda = \frac{1 \text{ tube breach failure per core}}{[(91 \text{ tubes/fuel assembly})(53 \text{ fuel assembly/core}) + (61 \text{ tubes/control rod})(12 \text{ control rods/core})](5{,}238 \text{ hr})}$$

$\lambda = 1/(2.91E+07 \text{ tube-hr})$
$\lambda = 3.4E-08 \text{ failures/tube-hr}$

One tube is a total 0.441 m in length (0.44 m/tube) (Stevenson 1987) so

$\lambda = (3.4E-08 \text{ breach failures/tube-hr})/(0.44 \text{ m/tube})$
$\lambda = 7.8E-08/\text{m-hr}$ as a maximum likelihood estimator for the tube failure rate

The failure rate was calculated based on one core's annual operation time and one core's failures rather than collecting the entire life history of EBR-II fuel. This was done for two reasons: (a) documentation from the 1960s to 1990s is difficult to obtain and is potentially incomplete on all cracked fuel tubes and (b) later life cores tested experimental fuel loadings with different ferritic-martensitic steels (i.e., HT-9) and stainless steel cladding materials, including SS316 and D9, with various metallic U-Zr fuels (Lahm et al. 1993).

Table 5. EBR-II capacity factors

Operating Year	Capacity Factor (%)
1965	26.4
1966	43.0
1967	20.1
1968	41.8
1969	42.4
1970	57.9
1971	39.1
1972	46.9
1973	49.9
1974	58.7
1975	66.1
1976	76.9
1977	71.5
1978	72.8
1979	71.1
1980	77.1
1981	73.0
1982	62.3
1983	65.5
1984	65.9
1985	75.0
1986	71.9
1987	81.3
1988	79.4
1989–1994	No published data were located, but the plant continued operating in a similar fashion as the 1980s. The given average is likely a low value.
Average capacity factor for 1965-1988	59.8

Data taken from (Perry et al. 1978; Perry et al. 1982; Chang 1991).

No failure rate should be given without its associated error. Atwood et al. (2003) give the Chi-square distribution to estimate error bounds for failure rates. The 95% and 5% bounds for a 90% confidence interval were used as customary error bounds.

95% upper bound failure rate, $\lambda_{95\%} = \chi^2(2x+2)/2T$

where

χ^2 = the Chi-square distribution for the 95% tail

x = the number of failures

T = the total component population operating time in unit-hr

and

5% lower bound failure rate, $\lambda_{5\%} = \chi^2(2x)/2T$

In these two calculations, $x = 1$ and the total operating time $T = 2.91E+07$ tube-hr.

The Chi-square distribution values are taken from a table in O'Connor (1985). The Chi-square value for a 95% bound with 2(1) + 2 = 4 degrees of freedom is 9.49. The Chi-square value for a 5% bound with 2 degrees of freedom is 0.103. Therefore,

95% upper bound faiure rate, $\lambda_{95\%} = \chi^2(2x+2)/2T = 9.49/[2(2.91E+07\ tube\text{-}hr)]$

$\lambda_{95\%} = 1.6E-07/tube\text{-}hr$

5% lower bound failure rate $\lambda_{5\%} = \chi^2(2x)/2T = 0.103/[2(2.91E+07\ tube\text{-}hr)]$

$\lambda_{5\%} = 1.8E-09/tube\text{-}hr$

Next, the basic failure rate requires adjustment for several factors: the operating temperature difference, flow media factor, radiation damage, and wall thickness (Cadwallader 2010). Vibration is also treated. The following subsections address these parameters.

3.2 Failure Rate Modifiers

The EBR-II data provide a basic failure rate for tube breach. However, the EBR-II operating conditions are very different from the ITER IVC operating conditions so failure rate modifiers will be used to adjust the parent failure rate to apply it to the new ITER application.

3.2.1 Operating Temperature

The EBR-II core operated at a temperature of 883°F or 746 K (Koch 1988). The ITER in-vessel coils operate at about 423 K (150°C) but could occasionally be baked at 240°C (Heitzenroeder 2012b). The coil is not in operation during bakeout. An Arrhenius exponential equation method to account for the temperature difference is given in Cadwallader (2010):

$\lambda_2/\lambda_1 = \exp[B \times (1/T_1 - 1/T_2)]$

where subscript 1 is the known failure rate and operating temperature (T_1 = 746 K) and subscript 2 is the unknown failure rate and new operating temperature (T_2 = 423 K) of the other application. From Cadwallader (2010), the B constant can be taken as 1623.39 K from operating experience data for steel piping. The new failure rate for the lower temperature of operation is

$$\lambda_2/(7.8E\text{-}08/hr\text{-}m) = \exp[1623.39K \times (1/746 - 1/423)]$$
$$\lambda_2/(7.8E\text{-}08/hr\text{-}m) = \exp[1623.39K \times (0.00134 - 0.00236)]$$
$$\lambda_2 = (7.8E\text{-}08/hr\text{-}m)\ \exp[-1.6625]$$
$$\lambda_2 = (7.8E\text{-}08/hr\text{-}m)(0.1897)$$
$$\lambda_2 = 1.5E\text{-}08/hr\text{-}m$$

Thus, the operating temperature adjustment to the basic failure rate to account for the lower ITER operating temperature gives a new point estimate failure rate value of 1.5E−08/hr-m. Given the ranges of temperature adjustment factors given for some aerospace equipment (NASA 1971), this factor of 0.1897 is reasonable.

3.2.2 Wall Thickness

There is a substantial difference in wall thicknesses and diameters between EBR-II cladding and the IVC. The EBR-II cladding tubes had a 0.3 mm thick wall and the ITER IVC uses a 2 mm thick wall (see Figure 1). The EBR-II cladding tubes were 3.66 mm outside diameter and the IVC is 59 mm. The Thomas Method (Thomas 1981) gives the pipe leakage failure rate, P_{leak}, as being proportional to length, diameter, and wall thickness:

$$P_{leak} \approx (L \times D)/t^2$$

where

L = length of pipe

D = diameter of pipe

T = thickness of pipe wall.

Thomas states that for prevailing pipe fabrication technology, the pipe has fewer but larger size flaws as the pipe wall thickness increases. For two applications where the pipe wall thickness and diameter vary greatly, if the pipe length is held constant and the change in the P_{leak} is sought for two different pipes, then the ratio of P_{leak} for Pipe 1 (P_1) to Pipe 2 (P_2) is

$$P_1/P_2 = [(L_1 \times D_1)/t_1^2]/[(L_2 \times D_2)/t_2^2]$$

The length L is considered to be constant because the failure rate is per unit length and therefore it cancels out of the equation, leaving

$$P_1/P_2 = [D_1 \times t_2^2]/[D_2 \times t_1^2]$$

For t_1 = 0.3 mm thick and D_1 = 3.66 mm stainless steel EBR-II tubing and t_2 = 2 mm thick and D_2 = 59 mm IVC tubing, the equation to find the final failure rate λ_2 is

$$k_{wallthickness} = \lambda_1/\lambda_2 = [D_1 \times t_2^2]/[D_2 \times t_1^2]$$

$$k_{wallthickness} = [3.66mm \times (2mm)^2]/[59mm \times (0.3mm)^2]$$
$$k_{wallthickness} = 0.689$$

The failure rate multiplier to adjust for wall thickness and diameter is 0.689.

3.2.3 Flow and Flow Media

The EBR-II used sodium coolant flowing at 23.8 ft/s (7.25 m/s) through the core (Koch 1988). Each fuel assembly had an outer stainless steel duct so that the flow was channeled vertically through the element rather than horizontally across several elements. The flow environment was typically low corrosion. It has been stated that the chalk marks left by constructors inside the piping in the 1960s were still legible when the reactor piping was investigated after decommissioning in the late 1990s. The stainless steel inner wall of the IVCs will not see any flow (see Figure 1) because there is an inner tube of copper that carries the water coolant. The IVC stainless steel pipe sees vacuum on the exterior and solid magnesium oxide insulation on the interior as a static configuration. The EBR-II cladding had very low, or even non-existent, flow corrosion issues (Walters 1999). Therefore, no correction to the EBR-II data is needed to apply it to the IVC. Thus, the flow and flow media correction factor is 1.0 and there is no change to the point estimate failure rate value.

3.2.4 Radiation Environment

The neutron radiation flux levels in the EBR-II core and the ITER IVCs in the vacuum vessel are similar, although EBR-II values were higher so
(1E+15 n/cm^2-s EBR-II flux) × 5,238 hr/core × 60 min/hr × 60 s/min = 1.9E+22 n/cm^2 fast neutron fluence on the cladding stainless steel. Both applications are fast neutron and gamma ray environments, and a fast fission reactor core is the highest neutron energy available on a large scale to approximate ITER conditions. The ITER neutron flux is stated to be an instantaneous average of at least 0.5 MW/m^2 (Chiocchio 2010), which is about 2.2E+13 n/cm^2-s of fast neutrons, assuming all neutron energy is given up in the blanket. The IVC VS coil fluence was calculated to be a peak of 3.6E+20 n/cm^2 (Sawan 2012). While ITER is a lower fluence than EBR-II, the EBR-II fuel cladding is the best large-scale usage of stainless steel in a high radiation environment so this inference of EBR-II stainless steel to the IVCs is the best presently known. The radiation damage correction factor is assumed to be 1.0 because the parent failure rate comes from a more harsh environment. There is no change to the point estimate failure rate value from the EBR-II cladding to apply to the IVC conditions.

3.2.5 Vibration Environment

A literature search for the flow-induced vibration characteristics of EBR-II fuel was not successful. However, the MONJU reactor, a similar facility, did report on tests of its fuel elements. The natural vibration frequency was 16 Hz under flow and the peak displacement was 0.05 mm (Sato 1977). EBR-II may have been lower values, primarily because of a lower coolant flow velocity used in the lower power EBR-II. Both reactors had very similar fuel design and they are sodium-cooled, but MONJU is a larger core at 700 MW thermal power (versus 62.5 MW in EBR-II) and may have had a higher flow velocity than EBR-II. Wowk (1991) gives an equation to relate gravities (g), frequency (Hz), and displacement (D), $D = 9.78(g)/(Hz)^2$. D is in inches, g is the number of gravities, and frequency is in Hz. For D = 0.05 mm or 0.00197 in. and 16 Hz, the gravities acceleration = 0.05 and the root mean square value of gravities acceleration = 0.035.

The IVC coil frequency is expected to be 5 Hz (Daly et al. 2012), and the gravities are not known but are expected to be much less than ITER's rare seismic events. An ITER seismic level 2 (SL-2) event gives vacuum vessel radial acceleration of 4.6 m/s^2 (0.47 gravities) at the supports, toroidal acceleration of 1.47 m/s^2 (0.15 gravities) at the bottom of the vessel, and vertical acceleration of 27.8 m/s^2 (2.8 gravities) at the inboard vessel wall (Martinez 2012). Operational vibrations must be less than rare SL-2 earthquakes, which are severe events. A value of 1 gravity peak acceleration at 5 Hz would be 10 mm amplitude, more than expected, but a 1 gravity peak or 0.707 g_{rms}, is assumed for the IVC coils in typical operation as a conservatively high overestimate. This is greater than the expected vibration in the sodium-cooled reactor core.

The FIDES (2010) relation for a failure rate modifier and vibration (Basquin's Law) is

$$AF = (g_{rms}/g_{rms0})^{1.5}$$

FIDES recommends 0.5 g_{rms} for aluminum and copper. Stainless steel should have greater vibration tolerance than aluminum or copper, so the recommended 0.5 g_{rms0} will be used with the assumed 0.707 g_{rms}, so AF = $(0.707/0.5)^{1.5}$ gives a failure rate modifier of 1.68.

3.3 Final Failure Rate Value

The EBR-II failure rate modifiers have been calculated and are shown in Table 6. The failure rate and its confidence bounds have been adjusted to account for the IVC environment.

Table 6. Stainless steel tubing failure rates and adjustment factors

Calculated Failure Rate and Failure Mode from EBR-II (/hr-m)	Operating Temperature Factor	Wall Thickness Factor	Flow and Flow Media Factor	Radiation Factor	Vibration Factor	Resulting Value for IVC Use (/hr-m)
Mean 7.8E−08 breach	0.1897	0.689	1.0	1.0	1.68	1.7E−08
95% bound 1.6E−07 breach	0.1897	0.689	1.0	1.0	1.68	3.5E−08
5% bound 1.8E−09 breach	0.1897	0.689	1.0	1.0	1.68	3.95E−10

3.4 Other Stainless Steels

Please note that in 1970, the Mark-I fuel (with SS 304L) was redesigned to Mark-II fuel for use in EBR-II. Initially the staff continued to use SS 304L in Mark-II fuel, but then SS 316 was also used in Mark-II, Mark-IIC, and Mark-IICS fuel (Lahm et al. 1993). 30,000 Mark-II cladding tubes were used with excellent results (that is, high reliability of less than one tube failure per core) when uranium burnup was held to 8 atom% (Walters 1999). From that experience, we can conclude that the dimples in the tube walls did not always cause a stress riser for crack growth. Given the discussions by Walters (1999) and Lahm et al. (1993), it is reasonable to assume that the cladding performance was good across each of the cladding materials. Therefore, the basic "per core" failure rate of the cladding given above should apply to any of the austenitic stainless steel cladding materials—304, 316, cold worked 316, and cold worked D9, as well as the ferritic steel HT-9.

The average EBR-II core fast neutron fluence was ≈ 1.9E + 22 n/cm^2. Lahm et al. (1993) stated that all of the advanced fuel element designs tested had demonstrated the ability to exceed the exposure capability of the standard fuel assembly hardware, which had a neutron fluence limit of 9.3E + 22 n/cm^2 at E_n > 0.1 MeV. Part of this hardware, the stainless steel 304 flow duct fitted around the fuel assembly, gave the most radiation damage issues with swelling. EBR-II cladding steels did suffer embrittlement and loss of ductility but these effects did not seriously impede operations. Swelling and irradiation-induced creep also occurred and were persistent problems that required operating adjustments (Walters 1999). Nonetheless, the cladding and the weld caps on the fuel cladding tubes withstood the EBR-II core

environment with very few breaches. If the peak fast neutron fluence for IVC coils is 3.6E + 20 n/cm^2, the stainless steel should be able to tolerate this radiation environment.

The EBR-II cladding tube failure rate of 7.8 E−08/hr-m is a higher value than the failure rates for stainless steel piping. Buende et al. (1991) and Schnauder et al. (1997) gave some values for pipes and welds in fusion environments. Their reported failure rates are one to two orders of magnitude lower than the cladding tube failure rate; however, with failure rate adjustments, the values from different studies have less variance. It is possible that if all of the EBR-II data and the Fast Flux Test Facility cladding tube data were compiled and analyzed, then the cladding failure rate might be reduced. Given the cladding performance, it is reasonable to expect that the numerator of the λ calculation (the failure count) would increase slowly while the denominator would increase more rapidly by collection of a larger data set if EBR-II had continued to operate. This type of performance has been seen with light water fission reactors and zirconium alloy cladding, where failures actually decreased while operating time and fluence increased in the 1990s. Perhaps the calculated failure rate for stainless steel is not the best approximation of a constant failure rate for matured stainless steel components. However, the 7.8E−08/hr-m failure rate is statistically valid and is the result of known operating experience. When this value is modified to account for the less harsh ITER operating environment, the result is a lower value of 5.6E−10/hr-m. This adjusted failure rate also includes the EBR-II cladding welds—a small arc weld on one tube end cap and an electric discharge fusion weld on the other tube end cap.

The EBR-II failure rate for the stainless steel tubes, 7.8E−08/hr-m, was attained by adhering to the following requirements. The tubing was procured to a strict specification and was required to be mandrel drawn to dimension and then 100% of the tubes were tested for wall defects by a pulsed eddy-current system. Tube samples were taken from each batch and tested to verify that they met strength requirements. One end of the tube had a plug called a tip. The tips were investment-cast stainless steel of the same grade as the tubes and were inspected for dimensional conformance to the specification by the use of contour projection. The tip was inserted and machine arc-welded to the tube end. The welds were 100% visually examined and 100% helium leak tested. The tubing was also 100% examined for diameter by use of an air gauge, and the tubing surface was 100% visually examined for defects. The tubes were cut to length with square ends to obtain precise dimensions. The other end of the tube was not sealed with a tip; rather, it was sealed with a restrainer plug. The restrainer plug had a rod inside the cladding tube to keep the metal fuel rod in a specified location (and neutron-induced swelling was accounted for in the restrainer design). The outside end of the plug had a small axial protrusion in its center. In an inert atmosphere, a condenser discharged onto the protrusion through a tungsten electrode. This energy fused the end of the plug to the tube. An essentially leak-free hemispherically welded end was obtained in this manner. A helium test was performed on each tube—the tube was placed in a chamber, the chamber was quickly pressurized with helium, and the pressure decay curve was observed for a few minutes. No pressure decay in the chamber meant no leakage of helium into the fuel tube (Stevenson 1987). This 100% inspection and stringent quality control was instrumental in achieving < 1 failed cladding tube per core at EBR-II.

In another study, a failure rate for stainless steel vacuum piping was calculated as 1.8E−12/hr-m (Cadwallader 2010). The difference between that result and the IVC result is noted. The vacuum piping was a very different application. It had near room-temperature operation, a very mild (noncorrosive) flow environment, a mild radiation environment (low beta-gamma radiation and very little neutron fluence), and the piping was 6.3 mm (Schedule 20) wall thickness typical of vacuum piping. Each of these failure rates was calculated for a specific application, so there is no easy comparison between values. The failure rate values found in Table 6 are recommended for the ITER IVCs.

The stainless steel material used for EBR-II cladding allows for a comparison of that highly irradiated steel to very mildly irradiated stainless steel used in power plant piping. From Cadwallader (2010), the stainless steel piping failure rate is 3.7E−11/hr-m as a mean value. This value comes from large, stainless steel feedwater piping in a nuclear power plant that operates at about 215°C (488 K) and is exposed to

some beta-gamma radiation and little neutron fluence. The piping has high flow and modest vibration. The piping headers are 508 mm (20 in.) outside diameter or perhaps larger, but most of the piping is on the order of 304.8 mm (12 in.) diameter and 9.53 mm (Schedule 40, 0.375 in. thickness) wall thickness. This stainless steel usage is very different from that of the EBR-II fuel cladding. Comparing more analogous components would be highly preferred but this is the only stainless steel data available to allow for a crude comparison. The radiation *k* factor can be found from these two stainless steel failure rates:

$$(\text{nuclear power plant } \lambda)(k_{temperature})(k_{wall\ thickness})(k_{flow})(k_{radiation})(k_{vibration}) = \text{EBR-II } \lambda$$

With the Arrhenius equation from Cadwallader (2010) for temperature adjustment and the two operating temperatures of 488 K and 746 K, the *k* factor is 3.2. The flow factor is assumed to be 1.0 given that the corrosion environment of stainless steel with feedwater is reputed to be low (Shah 1993) and the EBR-II stainless cladding had low corrosion in sodium coolant. The vibration *k* factor is taken to be 1.68 as described elsewhere in this report. The wall thickness factor for tube thickness and diameter is

$$k_{wallthickness} = \lambda_1/\lambda_2 = [D_1 \times t_2^2]/[D_2 \times t_1^2]$$

$$k_{wallthickness} = [3.66mm \times (9.53mm)^2]/[304.8mm \times (0.3mm)^2]$$

$$k_{wallthickness} = 12.1$$

Thus,

$$(3.7\text{E}{-}11/\text{hr-m})(3.2)(12.1)(1)(k_{radiation})(1.68) = 7.8\text{E}{-}08/\text{hr-m}$$

Using these estimates for the *k* factors, the radiation damage *k* factor is found to be 32.4, which is higher than was expected but is plausible. The reader will recall that these are very different applications of stainless steel and the comparison is crude so some variation in results is expected. The analyst judgment value of 10 for the radiation damage *k* factor used in other sections of this report is perhaps low but is a reasonable starting value of the correct order of magnitude. Other metals would need to be compared in a similar fashion to allow an increase of the radiation damage factor to a higher total value.

3.5 Conclusions

The ITER IVCs require a failure rate for the outer stainless steel tube that contains the magnet. The most applicable operating experience was considered to be from the stainless steel cladding on fission reactor fuel in the EBR-II fast reactor. An examination was made of the published data available and a failure rate for cladding tube breach was calculated on a per-core basis. This failure rate should apply to any of the austenitic materials that were used as cladding material in EBR-II. The IVC designer would have to account for radiation-induced swelling and other material damage effects such as ductility loss. If the IVC is going to experience a lower fluence than initially believed, then the EBR-II stainless steel had a more severe environment and the IVC radiation effects would be less pronounced than those in the fission cladding. The EBR-II cladding failure rate was modified by temperature, wall thickness, and vibration to apply to the IVC. The base values, modifiers, and resulting values for stainless steel tubing breach, which includes the tube welds, are given in Table 6. The adjusted values for the IVCs are 3.95E−10/hr-m lower 5% bound, 1.7E−08/hr-m mean, and 3.5E−08/hr-m upper 95% bound.

4. CuCrZr Piping Failure Rate

The ITER IVCs with CuCrZr conductor are used for mitigating plasma ELMs. The Tore Supra tokamak at Cadarache, France has used this material as an actively cooled heat sink in their toroidal pump limiter. The experiences of this limiter will be used to develop a failure rate for CuCrZr in the IVCs. The coil in question is shown in Figure 2. The CuCrZr is 6.35 mm thick in a pipe form. The CuCrZr carries electrical current and is cooled by flowing water. The operating temperature is 150°C.

4.1 Operating Experiences

Uses of CuCrZr were sought to develop a failure rate. Tore Supra was identified as having used CuCrZr in quantity. The machine was shut down in 2000 to install a toroidal pumped limiter (TPL) that uses this copper alloy. The tokamak restarted in 2002 (Magaud et al. 2007). The operating time, number of components, and number of failed components are described below.

4.1.1 Operating Time

The Tore Supra operating time has been collected by Vallet (2007). The graph in Figure 5 shows the operating days per year as well as in-vessel water leaks. The operating days in 2002–2007 are 54 + 52 + 64 + 72 + 92 + 32 = 366 days. Bucalossi and the Tore Supra Team (2010) gave the operating days for 2008 as 60 days. Thus, 2002–2008 sums to 426 days. This gives a yearly average of 60.8 days/yr. Assuming that average for 2009–2010 gives an additional 121 days. A Tore Supra operating day is 12 hours (van Houtte et al. 1997). Therefore, the operating hours for the TPL are (426 d + 121 d)(12 hr/d) = 6,564 hr.

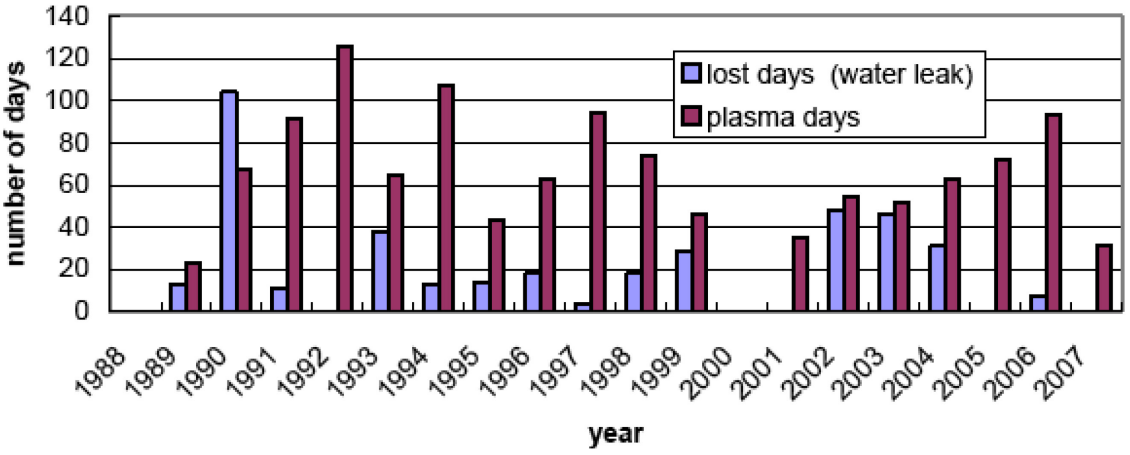

Figure 5. Tore Supra operating times (Vallet 2007)

4.1.2 Number of Components

The Tore Supra usage of CuCrZr is shown below in Figure 6. While it is labeled heat sink in Figure 6, the CuCrZr alloy is a structural material that not only conducts heat well but also withstands plasma forces. This use of CuCrZr is not as a magnet, instead it is a high heat flux component—but it is the best operating experience data set on a fairly large amount of CuCrZr in a fusion environment available at present. Each TPL finger element is about ≈ 0.4 m in length and 2.5 cm wide and there are two cooling channels in each finger (Schlosser et al. 1998). There are 574 of these units in the Tore Supra TPL (Cordier 2003). They are cooled by water at 40 bar and 150°C (Garin 2000) and ≈ 10 m/s water flow in the fingers (Cordier et al. 2000). The fingers were helium leak tested in place. The maximum allowed

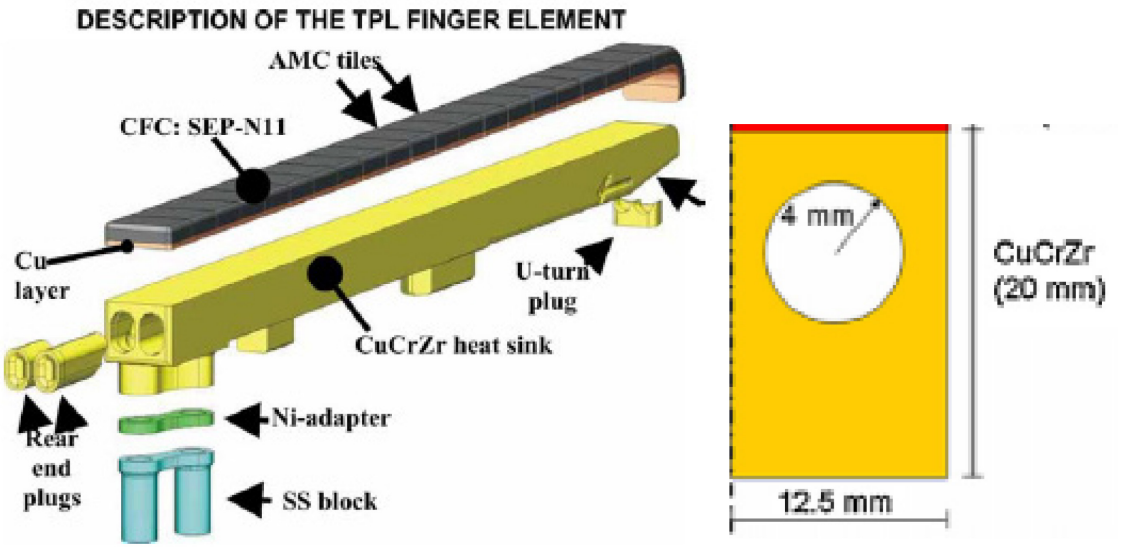

Figure 6. An exploded view of a Tore Supra toroidal pump limiter "finger" element with CuCrZr (Grosman and Tore Supra Team 2005; Chevet et al. 2009)

leak rate is 5E−10 Pa-m^3/s at room temperature with helium pressure of 6 MPa in the cooling piping and 5E−09 Pa-m^3/s at 200°C with helium pressure at 4 MPa in the cooling piping (Cordier et al. 2000). The specifications for Tore Supra CuCrZr are given in Table 7.

The dimensions of each CuCrZr finger were given by Chevet et al. (2009). The flow channel is 4 mm radius, and the CuCrZr is 20 mm tall, 25 mm wide, and 495 mm long. The CuCrZr wall thickness is 2 mm and 2.5 mm at a minimum across the width of the block (see Figure 6), and the walls are thicker over the height of the block. This flow channel is bored out of a solid block rather than tube construction. While not a tube, it is the best data set available for determining a pipe failure rate because it is the actual alloy material rather than an inference of steel or other pipe material to CuCrZr. The 2.5 mm will be used for the wall thickness failure rate modifier because selecting the thicker wall will give a more conservatively small modifier than assuming the smallest dimension that would give a larger modifier. With 574 fingers that have two flow channels of 0.495 m length, the total length of CuCrZr is (574 finger units × 2 channels/unit × 0.495 m/channel) = 568 m. Therefore, there is a total length of 568 m of CuCrZr in use in Tore Supra.

4.1.3 Number of Failures

Magaud et al. (2007) stated that in 4 years of operation from the 2002 startup with the TPL, no evidence of defects had been observed. This is interpreted to mean there were no failures of the TPL units in that time. No TPL failures in 2002 have been discussed in the literature so it is assumed there were no leaks or other faults upon initial startup for the one campaign in 2002. Vallet (2007) reported the water leaks inside Tore Supra and none of these were from the TPL through 2006. Cai et al. (2012) described investigations on the TPL for tile bonding from 2002 to 2010. There was no mention of CuCrZr problems (warping or leaking) in conjunction with tile debonding and overheating. Therefore, it is assumed that these CuCrZr heat sinks have operated without failure through 2010.

Table 7. Materials parameters for Tore Supra CuCrZr (Lipa et al. 2005)

Parameter	Values				
Chemical composition (wt%)	Cr is 0.6 to 0.8	Zr is 0.1 to 0.2	Oxygen ≤ 25 µg/g	Hydrogen ≤ 10 µg/g	Total impurities ≤ 0.15
Mechanical properties at 20°C	Ultimate tensile strength ≥ 400 MPa	Proof stress 0.2% ≥ 280 MPa	Elongation 18%	Brinell Hardness ≥ 130	
Mechanical properties at 400°C	Ultimate tensile strength ≥ 210 MPa	Proof stress 0.2% ≥ 170 MPa	Elongation 16%		
Delivery state	Age hardened				
Microstructure (grain-size)	≤ 200 µm				
Electrical conductivity ($m/\Omega mm^2$)	≥ 45				

4.1.4 Failure Rate Calculation

To calculate a failure rate with no failure events in the time period, the method by Atwood et al. (2003) is used. The average failure rate would be $\lambda = 0.5/T$, where T is the total operating time of the set of components. In this case, $\lambda = (0.5)/(568\ m \times 6{,}564\ hr) = 1.3E{-}07/m\text{-}hr$. This failure rate applies to all failure modes equally because no mode of failure was manifest in an actual failure. Therefore, this failure rate applies to small leaks, large leaks, rupture, and plugging. The upper and lower bounds are calculated by the Chi-square distribution (Atwood et al. 2003). The upper bound failure rate with a 95% Chi-square distribution and 2n + 2 degrees of freedom is $\chi^2(0.95,2)/2T$. The $\chi^2(0.95,2) = 5.99$ as found from Chi-square tables in O'Connor (1985). The upper bound failure rate calculation is $5.99/(2 \times 568\ m \times 6{,}564\ hr) = 8E{-}07/m\text{-}hr$. The Chi-square 5% lower bound failure rate calculation for zero failures uses 2n + 1 degrees of freedom. The $\chi^2(0.05,1) = 0.103$ as found from Chi-square tables in O'Connor (1985). The 5% lower bound failure rate is $0.103/(2 \times 568\ m \times 6{,}564\ hr) = 1.3E{-}08/m\text{-}hr$.

This "all modes" failure rate of 1.3E−08/m-hr from Tore Supra must be altered to account for different parameters so the failure rate can be applied to the ITER IVC coil. The Tore Supra and ITER IVC coil parameters are given in Table 8.

Table 8. Usage parameters for Tore Supra and ITER IVC CuCrZr

Operating Parameter	Tore Supra	ITER IVC
Operating temperature	150°C	150°C
CuCrZr wall thickness	2.5 mm	6.35 mm
CuCrZr radiation fluence	Low	3E+19 fast neutrons/cm^2 (estimated value)
Flow media	Water	Water
Flow velocity in one coolant channel	≈ 10 m/s	6 m/s ELM coils

4.2 Failure Rate Modifiers

The failure rate calculated from Tore Supra CuCrZr operating experience will be modified to account for the ITER IVC parameters of operating temperature, tube wall thickness, flow velocity/flow media, radiation fluence, and vibration. Each of these parameters is addressed below.

4.2.1 Operating Temperature

The Tore Supra TPL operated at a temperature of 150°C. This is the expected operating temperature of the ITER IVCs so there is no temperature adjustment factor required (factor = 1.0).

4.2.2 Wall Thickness

Using the Thomas method given by Cadwallader (2010) again gives

$\lambda_1/\lambda_2 = (t_2^2)/(t_1^2)$

Section 4.1.2 described that the CuCrZr is not a true pipe or tube so the form of this failure rate multiplier that accounts for the pipe diameter will not be used here.

If λ_1 is the Tore Supra component failure rate, t_1 = 2.5 mm for Tore Supra, and t_2 = 6.35 mm for the ITER IVC, then $\lambda_2 = \lambda_1[(t_1^2)/(t_2^2)]$

$$wall\ thickness\ modifier = (t_1^2)/(t_2^2)$$

$$wall\ thickness\ modifier = (2.5\ mm)^2/(6.35\ mm)^2$$

$$wall\ thickness\ modifier = 0.155$$

4.2.3 Flow and Flow Media

In this case, both the Tore Supra and IVC applications use water coolant so the failure rate adjustment factor is 1.0. The flow velocity factor should be accounted for because the ITER IVC operates at a high flow rate. The Tore Supra flow rate was ≈ 10 m/s. This is high for copper-based piping but apparently there have not been any deleterious effects over the approximately 10 years of Tore Supra operations.

Using the work by Chexal et al. (1998) as we did for copper in Section 2.2.3, we estimate that flow accelerated corrosion is increased by eight multiplicative factors:

- Temperature of the flow system
- Wall alloy content
- Mass transfer effect of protective oxide coating parting from the wall to the fluid
- Oxygen in the water effect
- pH of the water effect
- Geometry effect that promotes turbulence
- Void fraction in the water effect
- Hydrazine concentration in the water effect.

Each of these eight effects will be given an engineering judgment value based on what is known about the IVC system. As with the copper calculations, the failure rate modifier values for any one effect should be a maximum of $(6)^{1/8} = 1.25$. Each judgment on a modifier value is described below.

Temperature Effect. Temperature is a factor because the water solubility of the oxide layer that protects the pipe wall decreases with increasing temperature. For CuCrZr, a layer of black CuO (cupric oxide) forms to protect the pipe wall surface (Zheng et al. 2002). This behavior is the same as copper in water. Because CuCrZr composition is likely 0.6 to 0.9% Cr and 0.1% Zr with the balance being copper, the discussion of copper applies here. The solubility peaks of cupric and cuprous oxides in water are at a higher level than steel, more in the 150 to 350°C range with a high value at 250°C (Palmer and Benezeth 2004). Therefore, the low end 150°C to the peak of 250°C is the span of interest. Ratioing the 1.25 − 1.0 = 0.25 multiplier difference over the ΔT of 100°C gives 0.0025/°C in the range given by Palmer. The failure rate modifier for the IVCs will be assigned as 1.0025 because the IVC operating temperature of 150°C is just at the low end of the peak solubility temperature range.

Wall Alloy Effect. This factor was developed by Chexal et al. (1998) to take into account the elements of chromium, copper, and molybdenum in steel. The beneficial effect of chromium in CuCrZr (probably in the 0.6 to 0.9% range) is not as well defined as that of the corrosion-inhibiting effect of 0.1% Cr in carbon steel, but the chromium is expected to have a positive effect to reduce corrosion. This factor for the IVCs will be assigned as 1.0 to indicate there is no corrosion expected because of the alloy composition.

Mass Transfer Effect. This effect accounts for flow velocity, pipe diameter, coolant turbulence, and other hydrodynamic factors. The ELM IVC coils will have ≈ 6 m/s flow. Chexal et al. (1998) state that the mass transfer effect relation is $k = (Sh)(D)/(d_H)$. As with copper, ratioing the k numbers, $k_{IVC}/k_{Tore\ Supra}$ for the ITER IVC and Tore Supra conditions will give the failure rate modifier to the Tore Supra copper cooling channels to apply to the IVC. The D values will cancel out because both applications are the same material at the same operating temperature. The hydraulic diameter for the Tore Supra circular coolant channel is its diameter, $d_H = 0.008$ m (see Figure 6). For the hydraulic diameter of the IVC coil, d_H=diameter of the circular channel, or 0.03 m (see Figure 2).

If we create a ratio of the *Re* and *Sc* as we did with copper, the ratio will be

$$k_{IVC}/k_{Tore\ Supra} = \frac{[(0.023(Re)^{0.83}(Sc)^{0.33})(D)/(d_H)]_{IVC}}{[(0.023(Re)^{0.83}(Sc)^{0.33})(D)/(d_H)]_{Tore\ Supra}}$$

Cancelling out like terms in the numerator and denominator leaves

$$k_{IVC}/k_{Tore\ Supra} = \frac{[(v)^{0.83}/(d_H)]_{IVC}}{[(v)^{0.83}/(d_H)]_{Tore\ Supra}}$$

$$k_{IVC}/k_{Tore\ Supra} = \frac{[(6\ m/s)^{0.83}/(0.03\ m)]_{IVC}}{[(10\ m/s)^{0.83}/(0.008\ m)]_{Tore\ Supra}}$$

$$k_{IVC}/k_{Tore\ Supra} = 0.175$$

The Tore Supra CuCrZr failure rate should be multiplied by a factor of 0.175 to account for the mass transfer effects of flow accelerated corrosion for the IVC coils.

Oxygen Effect. No studies of CuCrZr resistance to dissolved oxygen in water were found, so copper studies will be used here. As a refresher from Section 2, Dortwegt and Maughan (2001) discussed that for water cooling of copper tubing, the corrosion from dissolved oxygen in water would peak at 200–300 ppb of oxygen, so operating at less than 50 ppb is advisable and close to 1 ppb oxygen is optimum. Zheng et al. (2002) suggested remaining below 30 ppb oxygen for brass and copper-nickel alloys—this is also good advice for CuCrZr. An assumption is made that the designers will specify to control oxygen concentration in the cooling water so that an optimum, or close to optimum, level will be present to maintain the protective cupric oxide and cuprous oxide (Cu_2O). Keeping oxygen low means accounting for radiolytic decomposition of water molecules and keeping the dissolved oxygen to low values that do

not corrode other flow loop materials such as the heat exchanger outside of the vacuum vessel. Recombining radiolytic oxygen by adding free hydrogen to the water, up to 2 ppm, may be necessary (Zheng et al. 2002). The 2 ppm is very high compared to typical water control standards. The oxygen concentration issue is assumed to be addressed by the hydrazine discussion below, so the modifier here will be assigned a value of 1.0.

pH Effect. Chexal et al. (1998) discusses that the rate of metal loss from the wall depends on solubility of the metal ions at the metal surface. For CuCrZr, acidic pH in the 1 to 5 range will not allow formation of stable surface oxides so the alloy surface will not form and keep a protective oxide layer (Kwok et al. 2009). Kwok et al. also discussed that at pH of 7, a passivation behavior is observed and becomes more pronounced as the pH increases to 10. Tore Supra operates at pH=7 when at operating temperature and at pH=9 at ambient (20°C) temperature. An assumption is made that the pH of the cooling water for the ITER IVCs is kept to an optimum value for CuCrZr, pH = 7 or higher. The pH factor is assumed to have been addressed in design and here it is given a value of 1.0.

Geometry Effect. In a carbon steel piping flow loop, this issue is generally concerning bends, elbows, control valves, and orifices in the flow stream that cause the water to impact or sweep over pipe surfaces downstream of these features. Corrosion is increased wherever the water is forced to turbulently sweep a pipe surface. The IVCs will have high turbulence due to flow velocity and four bends per IVC turn of 6 meters. Therefore, a maximum factor of 1.25 is assigned to account for the geometry effect.

Void Fraction Effect. The cooling water in the IVCs is pressurized, is expected to remain subcooled, and will have zero voids (that is, no two-phase flow). The factor for the IVCs will be assigned as 1.0 for the void fraction effect.

Hydrazine Concentration Effect. Noting the argument by Zheng et al. (2002) given earlier in this section, the cooling water in the IVCs may use injection of small amounts of hydrazine (N_2H_4) as a way to introduce hydrogen for recombining oxygen radicals in the cooling water. Tore Supra uses hydrazine to control the oxygen concentration to less than 50 ppb, but the level is not stated. Chexal et al. (1998) give some performance curves for various concentrations of hydrazine from 0 to 150 ppb with steel pipe. For 150°C operation, at 0 and 20 ppb hydrazine in water, the corrosion rate increases from 0.018 in./yr of wall thickness to 0.034 in./yr of wall thickness. The 20 ppb will be assumed here as the hydrazine needed in the IVCs. At 150 ppb hydrazine, the corrosion rate reaches 0.08 in./yr of wall thickness. Ratioing these corrosion rates gives

$$(0.034 - 0.018)/(0.08 - 0.018) = (x - 1)/(1.25 - 1)$$

$$x = 0.065$$

so the multiplier would be 1 + 0.065 or 1.065 to account for 20 ppb hydrazine.

The overall flow and flow media value is the product of one coolant factor and eight flow corrosion factors or (1 × 1.0025 × 1 × 0.175 × 1 × 1 × 1.25 × 1 × 1.065) = 0.234.

4.2.4 Radiation Environment

The Tore Supra tokamak operates with deuterium and protium fuel. As such, the neutrons produced tend to be in the 2 MeV range (Martin et al. 2001). Tore Supra still uses hands on, in-vessel maintenance to repair water leaks inside the vacuum vessel (Cordier et al. 2000; Samaille et al. 2005). Therefore, despite long pulses of 30 to 60 s and longer, the neutron fluence is modest in Tore Supra. The exact fluence value was not found in the literature, but given that hands-on work continues in the tokamak, the neutron activation, and hence the fluence, must be low. This is a case similar to the TFTR magnet coil copper discussed in Section 2: the neutron flux is low, much lower than expected in ITER. The base failure rate of the CuCrZr is from a fusion application where the neutron fluence was so low that the material is basically treated as not having been irradiated. Therefore, a radiation damage multiplier will

be needed to adjust the Tore Supra CuCrZr failure rate for the expected radiation damage to the ITER IVCs.

Zinkle et al. (2009) discussed the radiation damage processes that occur in structural materials at different temperatures and fluence levels. The radiation hardening and embrittlement are generally the low temperature phenomena of concern (that is, at less than 0.3 to $0.4T_{melt}$ when T_{melt} is in Kelvin) when neutron damage is > 0.1 dpa. Other phenomena emerge at higher temperatures and dpa levels. Because the melting temperature of CuCrZr is about 1353 K (1080°C), the same as copper, and the operating temperature is 423 K (150°C), then 423 K/1353 K = 0.313, which is within the lower end of the suggested temperature band for radiation hardening and embrittlement of the CuCrZr conductor. Therefore, factors to account for hardening and embrittlement will be used to modify the failure rate from the Tore Supra TPLs to apply to the ITER IVCs.

Heitzenroeder et al. (2009) gave an initial estimate of the neutron fluence as 1E+23 n/cm^2 for the IVCs. More recently, the neutron exposure estimate was reduced to on the order of 3E+19 n/cm^2 of fast neutrons (Heitzenroeder 2012b). Sawan (2012) calculated the fast neutron fluence ($E_n > 0.1$ MeV) for the most exposed ELM coils at 9.6E+19 n/cm^2 for the lower ELM coil and 1.5E+20 n/cm^2 for the upper ELM coil. Thus, the fast neutron radiation is ≈ 1E+20 n/cm^2.

The radiation damage will affect three important properties of the IVCs: the strength, embrittlement, and electrical resistivity. The magnets need to maintain structural strength to function properly and if radiation damage increases the electrical resistivity, then the magnets cannot operate at rated conditions over their service lifetime. These two properties will be addressed separately. As with copper, these failure rate modifiers will follow the approach used by Lauridsen et al. (1996). The radiation degradation factor, Δ, is

$$\Delta = (P_o - P_t)/(P_o - P_f)$$

where

P_o = value of a characteristic parameter of the material before radiation exposure

P_t = value of a characteristic parameter of the material after total radiation dose

P_f = value of the characteristic parameter of the material at failure.

As with copper, the factor of 10 will be applied to each mechanical property identified as an issue for radiation damage; this should result in a conservative estimate of the overall radiation damage to the CuCrZr. The radiation degradation factor is used as

Failure rate modifier for radiation damage $= 10^{(\Delta)}$

The properties of CuCrZr before and after irradiation are taken from a radiation damage study. Vandermeulen (1986) gave data points for cold worked and annealed CuCrZr before and after irradiation at 150°C. The composition of the CuCrZr irradiated sample was 0.86% Cr and 0.07% Zr, which varies from the composition given for the Tore Supra CuCrZr given in Table 8. Nonetheless, this irradiation study was performed at the operating temperature of interest, which is an important issue for radiation damage and damage healing, so these data will be used. The samples were irradiated to 5 dpa, or roughly 1E+21 n/cm^2, so the test fluence is higher than the IVC anticipated fluence. The yield strength for the CuCrZr samples before 5 dpa irradiation was 210 N/mm^2 (210 MPa), P_o= 210 MPa. This also varies from the data in Table 8, which was a 0.2% yield of 280 MPa. The yield strength was about 200 MPa after 150°C irradiation, P_t = 200 MPa. The parameter at component failure (P_f) is assumed to occur at stress = 2/3 × yield strength based on metals in the ASME Boiler and Pressure Vessel Code. In this case, that value is P_f = 133.3 MPa. With these data, Δ is

$$\Delta = \frac{(P_o - P_t)}{(P_o - P_f)}$$

$$\Delta = \frac{210\ MPa - 200\ MPa}{210\ MPa - 133.3\ MPa}$$

$$\Delta = 0.13$$

and

Failure rate modifier for radiation damage = $10^{(\Delta)}$
Failure rate modifier for yield strength radiation damage = $10^{(0.13)}$
Failure rate modifier for yield strength radiation damage = 1.35

Vandermeulen (1986) also gave plots for elongation of the CuCrZr samples that were irradiated, which accounts for embrittlement. Unirradiated CuCrZr was 29% elongation at temperature, $P_o = 0.29$. It is noted that this value varies from the Tore Supra value quoted in Table 7, but this CuCrZr alloy in this irradiation test is the closest material to IVC material found in the literature. At 150°C, the irradiated CuCrZr elongation was about 25% or $P_t = 0.25$. To set the elongation at failure for P_f, a conservative approach was used. Juvinall and Marshek (1991) suggested that a safety factor of 2 or even 3 be used with brittle material and that if elongation drops below 10%, the design should be examined for using a less brittle material. CuCrZr has less elongation overall than copper, and the safety factor cannot be chosen so conservatively in this case as it was for copper. A failure is assumed when elongation reduces to a value of 2 × 10% elongation or $P_f = 0.2$. In that case, Δ is

$$\Delta = \frac{(P_o - P_t)}{(P_o - P_f)}$$

$$\Delta = \frac{0.29 - 0.25}{0.29 - 0.20}$$

$$\Delta = 0.444$$

and

Failure rate modifier for radiation damage = $10^{(\Delta)}$
Failure rate modifier for elongation radiation damage = $10^{(0.444)}$
Failure rate modifier for elongation radiation damage = 2.78

Brager (1986) showed electrical conductivity values for fast neutron irradiated copper alloys. The conductivity did not begin to decline until the neutron fluence reached 1E + 22 n/cm^2. Brager stated that creation of nickel and zinc activation products in the copper matrix was a large factor in the electrical conductivity decrease. Eldrup and Singh (1998) stated that for 0.1 dpa neutron fluence (≈ 1E+20 n/cm^2 fluence) the electrical conductivity of copper alloys was > 91% of the unirradiated value. Less fluence would result in higher conductivity. At ≈ 1E+20 n/cm^2 fast neutron fluence, the electrical conductivity decrease is not expected to be very large, so the failure rate multiplier is assumed to be 1.0 for radiation effects on electrical conductivity.

The radiation damage multiplier accounts for copper strength change, copper embrittlement, and electrical resistivity and is 1.35 × 2.78 × 1.0 = 3.76.

4.2.5 Vibration Environment

Doré and Gauthier (2007) mentioned that the Tore Supra limiter had low frequency vibration on the order of 150 Hz with an amplitude of 0 to 1 micron. Assuming that this small amplitude is the peak amplitude, then the acceleration can be calculated from a formula given by Wowk (1991):

$A = 0.1022(f)^2(\text{peak displacement})$

where f is the frequency in Hz and displacement is in inches.

$A = 0.1022(150\ Hz)^2 \times (3.9E{-}05\ in.)$ or 0.09 gravities.

This is a low value for vibration and it does not seem to affect the reliability of the Tore Supra TPL fingers.

In Section 2 of this report, an assumption was made that the peak vibration amplitude in gravities for the IVC would be 1 gravity, or 0.707 gravities root mean square (g_{rms}). The IVC vibration frequency is expected to be 5 Hz (Daly et al. 2012). Basquin's Law is again used for CuCrZr as the failure rate modifier for acceleration factors as is the FIDES recommended 0.5 g_{rms}:

$AF = (g_{rms}/g_{rms0})^{1.5}$
$AF = (0.707/0.5)^{1.5}$
$AF = 1.68.$

4.3 Final Failure Rate Value

The Tore Supra CuCrZr piping failure rate from the in-vessel limiter is 1.3E−07/m-hr for all failure modes. That is, this failure rate would be applied to any failure mode, including small and large leakage, rupture, or blockage. The Chi-square 95% upper bound failure rate is 8E−07/m-hr. The Chi-square 5% lower bound failure rate is 1.3E−08/m-hr. The failure rate multipliers to apply to the Tore Supra CuCrZr failure rate for application to ITER IVCs are given in Table 9 below. The "all modes" CuCrZr piping failure rate to apply to the ITER IVCs is 0.23 × 1.3E−07/m-hr ≈ 3E−08/m-hr. The upper and lower bounds are 1.8E−07/m-hr and 3E−09/m-hr, respectively.

Table 9. CuCrZr piping failure rates and adjustment factors

Calculated Failure Rate and Failure Mode from Tore Supra (/hr-m)	Operating Temperature Factor	Wall Thickness Factor	Flow and Flow Media Factor	Radiation Factor	Vibration Factor	Resulting Value for IVC Use (/hr-m)
Mean 1.3E−07 all modes	1.0	0.155	0.234	3.76	1.68	2.98E−08
95% bound 8E−07 all modes	1.0	0.155	0.234	3.76	1.68	1.8E−07
5% bound 1.3E−08 all modes	1.0	0.155	0.234	3.76	1.68	2.98E−09

5. Inconel Tubing Failure Rate

The outer jacket of the IVC ELM coils is Inconel 625, UNS06625. Given that these coils are inside the vacuum vessel and the ITER neutron flux is a significant factor in material lifetime, an effort has been made to adjust an Inconel tubing failure rate for a nuclear environment. The IVCs need to withstand a 200°C bakeout temperature and a fast neutron fluence of 1E+23 n/cm^2 (Heitzenroeder et al. 2009). The preliminary coil configuration is shown in Figure 2.

This section focuses on the Inconel jacket of the ELM coil because there is a concern of release of foreign materials such as MgO or possibly water coolant into the vacuum vessel (Heitzenroeder et al. 2009). The largest use of Inconel pipe has been in the fission industry, primarily for tubing in steam generators.

The basic failure rate calculation is the number of failures in the set of components divided by the product of the total number of components and the time period of operation. That is,

λ = *(failure count)/(component count × operating time)*

Often, the number of failures is readily available from failure reports but the denominator information usually requires more effort to obtain from the component usage.

5.1 Operating Experiences

Marshall and Cadwallader (1994) gave a failure rate for Inconel 600 tubing in water that was calculated from fission industry steam generator experience. The average failure rate for leakage is 1.5E−07/m-hr, the 95% upper bound is 1.5E−06/m-hr, and the 5% lower bound would be 1.5E−08/m-hr. The tubing used in steam generators experiences high temperature operation at 315°C (600°F) and the average tube wall thickness is 1.27 mm (0.05 in.) and the outer diameter is 22.2 mm (0.875 in.). The differential pressure acting on the tubes is 8.3 MPa (1250 psia) (Masche 1971). A steam generator is depicted in Figure 7. The tube bundle has the Inconel alloy 600 tubes (NRC 2003). There are more than 2,000 tubes per bundle. The radiation environment is low dose, estimated at approximately 2 to 3 rem/hr (Prince 2012), mainly gamma-beta radiation from activated corrosion products in the water and perhaps some neutrons from the very tiny amounts of leaked fission products from the fission reactor's fuel. The neutron fluence is very low for steam generator tubes in fission power plants. It is assumed to be too low to result in any significant neutron damage so other studies will be used to estimate radiation effects. It is noted that Inconel alloy 600 is not exactly the same composition as UNS06625, but these are both Inconel alloys and there were no operating experience data available specifically for the Inconel 625 alloy. Inconel 600 data were found from large sets of tubes in dozens of power plants over more than 10 years of operation.

5.2 Failure Rate Modifiers

Next, the Inconel basic failure rate and its error bounds need adjustment for several factors: the operating temperature difference, wall thickness, flow media factor, radiation damage, and vibration. The following subsections address these parameters.

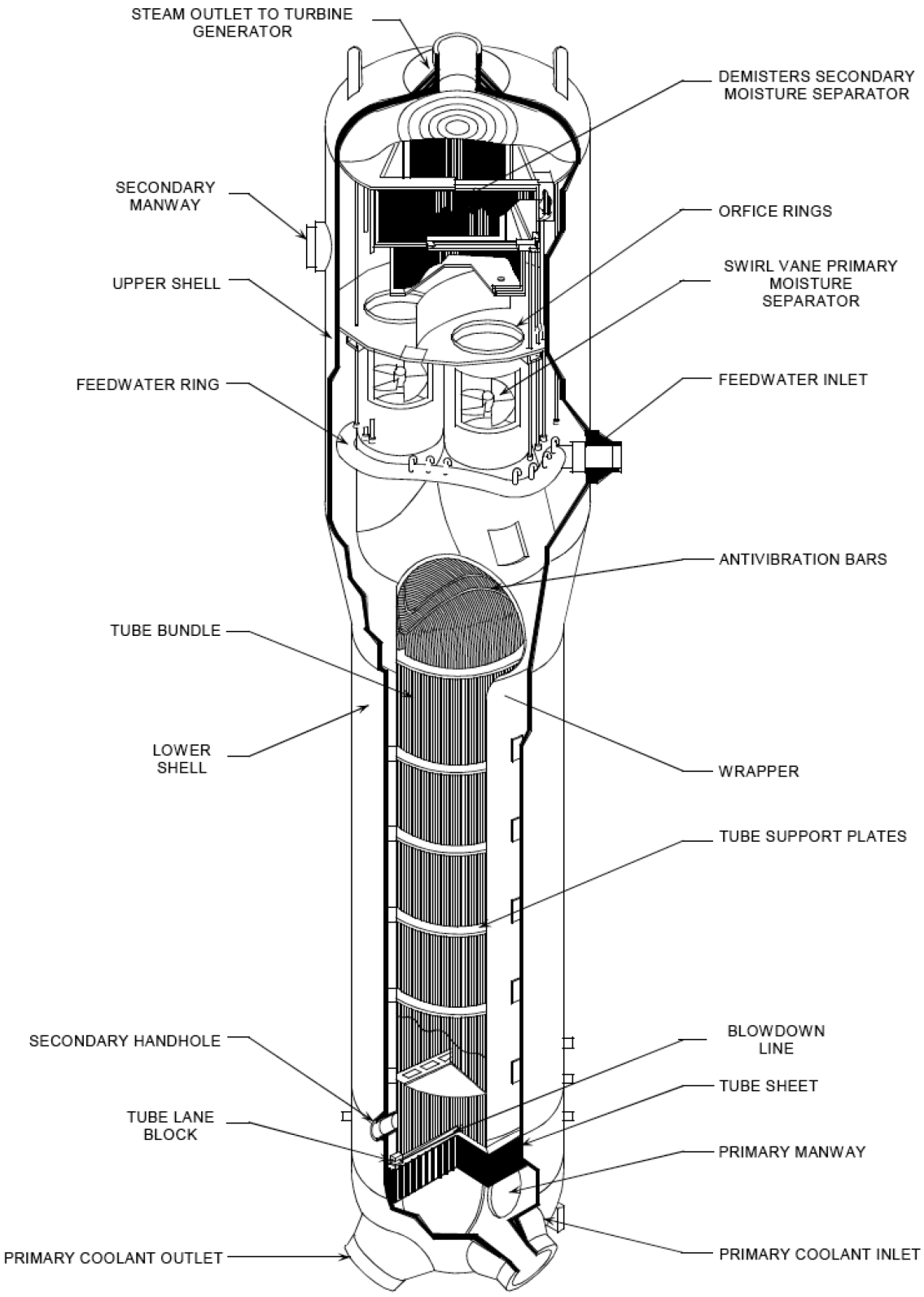

Figure 7. A cutaway view of a U-tube steam generator (NRC 2003)

5.2.1 Operating Temperature

Inconel is reputed to be a superalloy with good high-temperature strength and oxidation resistance (Schweitzer 2003) so it is used in high temperature applications, including gas turbines. The steam generator Inconel tubes routinely operated at 588 K (315°C) but Inconel has been used in power plants as a superheater that can reach three times that operating temperature. The ITER IVCs operate at only 423 K (150°C) but could occasionally be baked at 200–240°C (Heitzenroeder 2012b). The coil is not in operation during bakeout. Because the parent failure rate data from the fission industry originate from an application that is a higher temperature (315°C) than the IVC application (150°C), and noting that Inconel is reputed to be an alloy that can accommodate high temperature operation, to be conservative, no failure rate adjustment will be made for this high temperature alloy from the fission operating temperature to the IVC operating temperature. The operating temperature multiplier is assumed to be 1.0.

5.2.2 Wall Thickness

There is a substantial difference in wall thicknesses between Inconel tubes used in fission and the IVC. The Inconel tube walls in fission steam generators were 1.27 mm thick and the ITER IVC uses a 4 mm thick wall (see Figure 2). The Thomas method (Thomas 1981) gives the pipe leakage failure rate as being proportional to length, diameter, and wall thickness:

$$P_{leak} \approx (L \times D)/t^2$$

where

L = length of pipe

D = diameter of pipe

T = thickness of pipe wall.

Thomas states that for prevailing pipe fabrication technology, the pipe has fewer but larger size flaws as the pipe wall thickness increases. For two applications where the pipe wall thickness and diameter vary greatly, if the pipe length is held constant and the change in the P_{leak} is sought for two different pipes, then the ratio of P_{leak} for Pipe 1 (P_1) to Pipe 2 (P_2) is

$$P_1/P_2 = [(L_1 \times D_1)/t_1^2]/[(L_2 \times D_2)/t_2^2]$$

The length L is considered to be constant and therefore it cancels out of the equation, leaving

$$P_1/P_2 = [D_1 \times t_2^2]/[D_2 \times t_1^2]$$

For t_1 = 4 mm thick, D_1 = 59 mm IVC, and t_2 = 1.27 mm thick and D_2 = 22.2 mm steam generator tubing, the equation to find the k factor is

$$k_{wallthickness} = \lambda_1/\lambda_2 = [D_1 \times t_2^2]/[D_2 \times t_1^2]$$

$$k_{wallthickness} = [59mm \times (1.27mm)^2]/[22.2mm \times (4mm)^2]$$

$$k_{wallthickness} = 0.268$$

The failure rate multiplier to adjust for wall thickness and diameter is 0.268.

5.2.3 Flow and Flow Media

The Inconel tubes see flow in steam generators but the Inconel pipe does not see flow in the IVC application because it is an outer containment "jacket" pipe and not a cooling pipe. The fission-based failure rate includes many factors involving flow and corrosion (Tatone and Tapping 1989):

- Stress corrosion cracking from the tube interior = 44.8%
- Stress corrosion cracking from the tube exterior = 24.2%
- Fretting = 11.8%
- Pitting = 10%
- Phosphate wastage (phosphate erosion-corrosion) = 3.7%
- Denting = 0.5%
- Wall thinning = 0.4%
- Erosion = 0.4%
- Fatigue = 0.1%
- Mechanical damage = 0.3%
- Other failure mechanisms = 3.8%.

Most of these failure mechanisms are not present for this application where there is no cooling water, so these water-related failure mechanisms will be factored out. Retaining "other failure mechanisms," mechanical damage, fatigue, and denting failures, the failure rate adjustment factor becomes $1 - [0.448 + 0.242 + 0.118 + 0.10 + 0.037 + 0.004 + 0.004] = 0.047$. The correction to the fission failure rate data with its more harsh flow environment than the IVCs is 0.047. Thus, the flow and flow media multiplier to account for the Inconel not being under flow conditions is 0.047.

5.2.4 Radiation Environment

The literature was searched for Inconel alloy 600 irradiation studies because the parent failure rate is based on Inconel alloy 600. One such study was located (Wiffen 1978). The Inconel composition weight percent was Ni, 77.3%; Cr, 15.3%; Fe, 6.7%; Mn, 0.32%; Si, 0.28%; Ti, 0.18%; Al, 0.07%; and C, 0.05%. Unfortunately, the irradiation temperatures were 55°C and 300°C or higher. No study at 150°C was found. The fast neutron fluence (>0.1 MeV) gave the results listed in Table 10. The fast neutron fluence ($E_n > 0.1$ MeV) for the most exposed ELM coils are 9.6E+19 n/cm^2 for the lower ELM coil and 1.5E+20 n/cm^2 for the upper ELM coil (Sawan 2012). The irradiation study is a factor of 8 or more higher fluence. This is as close as the irradiation studies were found to come to the IVC conditions.

Table 10. Inconel 600 irradiation study results (Wiffen 1978)

Irradiation Conditions			Stress Test Temperature (°C)	Yield Stress (MPa)	Ultimate Tensile Strength (MPa)	Total Elongation (%)
Irradiation Temperature (°C)	Fast Fluence (per cm^2)	Displacements (dpa)				
55	1.24E+21	10.0	35	880	919	10.1
300	5.3E+21	4.3	300	924	925	4.2
Control sample, unirradiated			35	600	725	20.7
Control sample, unirradiated			300	540	700	19.2

The method given in Section 2 is used here to develop a multiplier for neutron irradiation effects on the Inconel:

Failure rate modifier for radiation damage $= 10^{(\Delta)}$

where

$$\Delta = \frac{(P_o - P_t)}{(P_o - P_f)}$$

P_o = *the initial material parameter of interest*
P_t = *the initial parameter value after irradiation*
P_f = *the initial parameter value at component failure.*

For Inconel, some unirradiated and irradiated mechanical properties are given in Table 10. The values at 55°C irradiation temperature will be used here because it is assumed that more defect healing will occur at the 300°C temperature than at the 55°C temperature (so the lower temperature should give a more conservative result). Two values will be evaluated: the yield strength and the elongation. These will account for irradiation damage and hardening/embrittlement. For yield strength, from Table 10 the control sample P_o is 600 MPa at 35°C. P_t is 880 MPa after irradiation at 55°C and the P_f is assumed to be 2/3 of the yield strength, based on the ASME Boiler and Pressure Vessel Code, or 400 MPa. Thus, $\Delta = [600 - 880]/[600 - 400] = -1.4$. The failure rate modifier for yield strength radiation damage is $10^{(-1.4)}$ or $0.0398 \approx 0.04$. This result is not surprising because the yield strength increased under irradiation. For elongation, the P_o is 0.207 and the P_t is 0.101. To set the elongation at failure, some guidance was used. Juvinall and Marshek (1991) stated that if elongation drops below 10%, the design should be examined for using a less brittle material so a failure is assumed when elongation reduces to a value of 10% elongation, or $P_f = 0.10$. This value is the lowest used for the set of the four IVC materials. The designers should evaluate this elongation value for Inconel; the irradiation test results are lower than expected. The elongation $\Delta = [0.207 - 0.101]/[0.207 - 0.10]$ or 0.9906 and the failure rate modifier for elongation radiation damage is $10^{(0.9906)}$ or 9.79. The combined radiation damage multiplier is $0.04 \times 9.79 = 0.39$.

5.2.5 Vibration Environment

Daly et al. (2012) had a concern that vibration of the IVC coils would be a reliability issue. The IVC coils are expected to have a 5 Hz vibration frequency. The steam generator tubes in fission reactors have been analyzed for vibration and these vibrate in the 6.5 to 9 Hertz range (King 1979). This would indicate that the vibration environment is not significantly different for the two applications of Inconel. It is noted that the fretting failure mode discussed in the flow and flow media multiplier is 11.8% of the failures of Inconel tubing in flow-induced vibration. Fretting is a failure where vibrating parts in contact (the steam generator tube and its guide rack) can microweld to each other and transmit stress, leading to a tube breach failure (Wulpi 1985). While the IVC vibration is from a different source and only has the other coil turns to contact rather than a tube bundle guide rack for a contacting part, this 11.8% will be included here to account for the vibration environment that is a similar value for the two applications. A multiplier of 1.118 will be applied to account for vibration of the IVCs.

5.3 Final Failure Rate Value

The Inconel failure rate from the fission industry has been adjusted to account for the IVC jacket environment. The error bounds require the same adjustment. All of these adjustments are shown in Table 11.

Table 11. Inconel tubing failure rates and adjustment factors

Calculated Failure Rate and Failure Mode (/hr-m)	Operating Temperature Factor	Wall Thickness Factor	Flow and Flow Media Factor	Radiation Factor	Vibration Factor	Resulting Value for IVC Use (/hr-m)
Mean 1.5E−07 leakage	1.0	0.268	0.047	0.39	1.118	8.2E−10
95% bound 1.5E−06 leakage	1.0	0.268	0.047	0.39	1.118	8.2E−09
5% bound 1.5E−08 leakage	1.0	0.268	0.047	0.39	1.118	8.2E−11

The ITER IVCs require a failure rate for the outer Inconel jacket pipe that contains the magnet coil. The most applicable operating experience was considered to be from the Inconel tubing used in fission reactor steam generators because this has been a large-scale, documented use of Inconel. An examination was made of the published data available and a failure rate for tube leakage was calculated in referenced work. The Inconel 600 alloy from fission is not exactly the same as the IVC alloy but this is the closest data that have been found and should be a good approximation of the Inconel 625 failure rate for the IVCs. The Inconel tube failure rate from fission was modified by temperature, irradiation, flow media, and wall thickness to apply to the IVCs. The base values, modifiers, and resulting values for Inconel tubing leakage (that is, cracking), including tube welds, are given in Table 11. The adjusted failure rate values for tube breach that are applicable to the IVCs are 3.1E−11/hr-m for the lower 5% bound, 8.2E−10/hr-m for the mean, and 8.2E−09/hr-m for the upper 95% bound.

6. References

ANSI, 2011, *American National Standard for Electric Connectors—Connectors for Use Between Aluminum-to-Aluminum and Aluminum-to-Copper Conductors Designed for Normal Operation at or Below 93°C and Copper-to-Copper Conductors Designed for Normal Operation at or Below 100°C*, ANSI C119.4-2011, Rosslyn, Virginia: National Electrical Manufacturers Association, March 30, Sections 6.7 and 6.8.

API, 2011, *Damage Mechanisms Affecting Fixed Equipment in the Refining Industry, Recommended Practice 571*, second edition, Washington, DC: American Petroleum Institute, April, Section 4.3.4.3.

Army, 1977, *Reliability, Maintainability, and Performance Issues in Hydraulic System Design*, USAAMRDL-TR-77-6, accession number ADA 045237, pg. 83.

Atwood, C. L., J. L. LaChance, H. F. Martz, D. J. Anderson, M. Englehardt, D. Whitehead, and T. Wheeler, 2003, *Handbook of Parameter Estimation for Probabilistic Risk Assessment*, NUREG/CR-6823, U.S. Nuclear Regulatory Commission, Washington, DC, September, pg. 6-6.

Bajenescu, T. I., M. I. Bazu, 1999, *Reliability of Electronic Components: A Practical Guide to Electronic Systems Manufacturing*, Berlin: Springer-Verlag, pp. 303–305.

Barnes, G. W., R. Pysher, J. Chrzanowski, and R. Woolley, 1995, "Operation of a Fluorinert Cooling System for the Toroidal Field Coils on TFTR," *Proceedings of the 16th Symposium on Fusion Engineering, Champaign, Illinois, September 30–October 5, 1995*, IEEE, pp. 520–521.

Barnes, G. W., G. R. Walton, and D. Bashore, 1994, "Operation of a Fluorinert Cooling System for the TFTR TF Coils and TFTR Coil Flowswitch Monitoring System Modification to Accommodate the TF Alternate Cooling System (Fluorinert)," *Proceedings of the 15th Symposium on Fusion Engineering, Hyannis, Massachusetts, October 11–15, 1993*, IEEE, pp. 329–332.

Brager, H. R., 1986, "Effects of Neutron Irradiation to 63 dpa on the Properties of Various Commercial Copper Alloys," *Journal of Nuclear Materials*, Vol. 141–143, pp. 79–86.

Bucalossi, J., and the Tore Supra Team, 2010, "Performance Issues for Actuators and Internal Components During Long Pulse Operations on Tore Supra," *IEEE Transactions on Plasma Science*, Vol. 38, pp. 393–399.

Buende, R., S. Fabritsiev, and V. Rybin, 1991, "Reliability of Welds and Brazed Joints in Blankets and Its Influence on Availability," *Fusion Engineering and Design*, Vol. 16, pp. 59–72.

Bush, S. H., M. J. Do, A. L. Slavich, and A. D. Chockie, 1996, *Piping Failures in United States Nuclear Power Plants: 1961–1995*, SKI-R-96-20, Stockholm, Sweden: Statens Karnkraftinspektion (the Swedish Nuclear Power Inspectorate), January.

Cadwallader, L., 2010, *Vacuum Bellows, Vacuum Piping, Cryogenic Break, and Copper Joint Failure Rate Estimates for ITER Design Use*, INL/EXT-10-18973, Idaho National Laboratory, June.

Cai, L., et al., 2012, "Evolution of the Bonding Defect Reported on the Tiles of the Toroidal Pumped Limiter of the Tore Supra Tokamak with Infrared Analysis," *Physica Scripta*, Vol. 85, doi 10.11088/0031-8949/85/01/015501.

Chang, Y. I., 1991, "Desirable LMR Design Features: Lessons Learned from EBR-II Operating Experience," *Conference: Potential of Small Nuclear Reactors for Future Clean and Safe Energy Sources, Tokyo, Japan, October 23–25, 1991*, ANL/CP-74230, CONF-9110153-1.

Chevet, G., J. Schlosser, E. Martin, V. Herb, G. Camus, and F. Escourbiac, 2009, "Initiation and Propagation of Damage in Actively Cooled CFC Armoured High Heat Flux Components in Fusion Machines," *Fusion Engineering and Design*, Vol. 84, pp. 586–589.

Chexal, B., et al., 1998, *Flow-Accelerated Corrosion in Power Plants*, EPRI TR-106611-R1, Palo Alto, California: Electric Power Research Institute, July, Section 7.

Chiocchio, S., 2010, *Project Requirements, ITER Document Management System*, ITER_D_27ZRW8v4.6, May 7, Section 6.7.

Cohen, A., and W. S. Lyman, 1972, "Service Experience with Copper Plumbing Tube," *Materials Protection and Performance*, Vol. 11, February, pp. 48–53.

Copper Development Association, 2010, *The Copper Tube Handbook*, Section III, available at http://www.copper.org/.

Cordier, J. J., 2003, "Preliminary Results and Lessons Learned from Upgrading the Tore Supra Actively Cooled Plasma Facing Components (CIEL Project)," *Fusion Engineering and Design*, Vol. 66–68, pp. 59–67.

Cordier, J. J., M. Chantant, Ph. Chappuis, and A. Durocher, 2000, "Ten Years of Maintenance on Tore Supra Actively Cooled Components," *Fusion Engineering and Design*, Vol. 51–52, pp. 949–954.

Daly, E. F., et al., 2012, "Update on Design of the ITER In-Vessel Coils," *20th Topical Meeting on the Technology of Fusion Energy, Nashville, Tennessee, August 26–30, 2012*.

Doré, P., and E. Gauthier, 2007, "Speckle Interferometry Diagnostic for Erosion/Redeposition Measurement in Tokamaks," *Journal of Nuclear Materials*, Vol. 363–365, pp. 1414–1419.

Dortwegt, R., and E. V. Maughan, 2001, "The Chemistry of Copper in Water and Related Studies Planned at the Advanced Photon Source," *Proceedings of the 2001 Particle Accelerator Conference, Chicago, Illinois, June 18–22, 2001*, IEEE, pp. 1456–1458.

Eldrup, M., and B. N. Singh, 1998, "Influence of Composition, Heat Treatment and Neutron Irradiation on the Electrical Conductivity of Copper Alloys," *Journal of Nuclear Materials*, Vol. 258–263, pp. 1022–1027.

Fabritsiev, S. A., and A. S. Pokrovsky, 1997, "The Effect of Neutron Irradiation on the Electrical Resistivity of High-strength Copper Alloys," *Journal of Nuclear Materials*, Vol. 249, pp. 239–249.

FIDES, 2010, *FIDES Guide 2009, Edition A, Reliability Methodology for Electronic Systems*, September, pp. 44–45, available at http://www.fides-reliability.org.

Fleming, K., and B. Lydell, 2006, *Pipe Rupture Frequencies for Internal Flooding PRAs, Revision 1*, EPRI 1013141, Palo Alto, California: Electric Power Research Institute, March.

General Atomics, 1989, *System Design Description of DIII-D*, GA-A19264, La Jolla, California: General Atomics, February, Chapter 3.

Gagliardi, M. G., and L. J. Liberatore, 2000, *Piping Handbook, 7th edition*, M.L. Nayyar (ed.), "Water Systems Piping," Chapter C1, New York: McGraw-Hill, pg. C-22.

Garin, P., 2000, "Ciel: Tore Supra's New Power and Particle Extraction Environment," *Fusion Engineering and Design*, Vol. 49–50, pp. 89–95.

Gettelfinger, G., F. Dahlgran, E. Perry, J Walsh, G. R. Walton, and H. Bush, 1989, "Oil as an Alternative Coolant for Use in the TFTR Toroidal Field Coils," *Proceedings of the 13th Symposium on Fusion Engineering, Knoxville, Tennessee, October 2–6, 1989*, IEEE, pp. 1181–1184.

Gill, K., R. Grabit, M. Persello, G. Stefaninni, and F. Vasey, 1997, "Gamma and Neutron Radiation Damage Studies of Optical Fibers," *Journal of Non-Crystalline Solids*, Vol. 216, pp. 129–134.

Gootgeld, A. M., 1995, "Cooling Water Conditioning & Quality Control for Tokamaks," *Proceedings of the 16th Symposium on Fusion Engineering, Champaign, Illinois, September 30–October 5, 1995*, IEEE, pp. 825–828.

Gootgeld, A. M., 1993, "Impact of Environmental Regulations on Control of Copper Ion Concentration in the DIII-D Cooling Water System," *Proceedings of the 15th Symposium on Fusion Engineering, Hyannis, Massachusetts, October 11–15, 1993*, IEEE, pp. 958–961.

Green, A. E, and A. J Bourne, 1972, *Reliability Technology*, London: Wiley-Interscience, pg. 567.

Green, D. W., and J. O. Maloney (ed's.), 1997, *Perry's Chemical Engineers' Handbook, seventh edition*, New York: McGraw-Hill Companies, Chapter 5, pg. 5–63.

Grosman, A., and the Tore Supra Team, 2005, "High Heat Flux Actively Cooled Plasma Facing Components Development, Realization and First Results in Tore Supra," *Fusion Engineering and Design*, Vol. 74, pp. 49–57.

Heitzenroeder, P. J., 2012a, Princeton Plasma Physics Laboratory, email communication, Subject: "Failure rates of pipes, bellows, etc. appropriate for the ITER In-Vessel Coils," March 26, 2012.

Heitzenroeder, P. J., 2012b, Princeton Plasma Physics Laboratory, teleconference communication, April 2, 2012.

Heitzenroeder, P. J., et al., 2009, *An Overview of the ITER In-Vessel Coil Systems*, PPPL-4465, Princeton Plasma Physics Laboratory, September.

Heitzenroeder, P. J., 1991, *Designing Magnetic Systems for Reliability*, PPPL-CFP-2469, CONF 910968-30, Princeton Plasma Physics Laboratory, January.

Hurh, P. G., 1999, *Microbiologically Influenced Corrosion in the Main Injector Magnet Low Conductivity Water System, case history and final recommendations*, MI-0254, Fermi National Accelerator Laboratory, March 4.

IEEE, 1984, *IEEE Guide to the Collection and Presentation of Electrical, Electronic, Sensing Component, and Mechanical Equipment Reliability Data for Nuclear-Power Generating Stations*, IEEE Std 500-1984, Institute of Electrical and Electronics Engineers, New York, December.

Joseph, G., 1999, *Copper, Its Trade, Manufacture, Use, and Environmental Status*, Materials Park, Ohio: ASM International, pg. 292.

Juvinall, R. C., and K. M. Marshek, 1991, *Fundamentals of Machine Component Design, second edition*, New York: John Wiley & Sons, Inc., pg. 224.

King, D. M., 1979, *Free Vibration Analysis of a Steam Generator Tube Bundle with and without Lateral Support*, UCID-18018, Lawrence Livermore Laboratory, April.

Kishimoto, H., M. Nagami, and M. Kikuchi, 1998, "Recent Results and Engineering Experiences from JT-60," *Fusion Engineering and Design*, Vol. 39–40, pp. 73–81.

Koch, L. J., 1988, *EBR-II, Experimental Breeder Reactor-II, An Integrated Experimental Fast Reactor Nuclear Power Station*, Argonne National Laboratory.

Kwok, C. T., P. K. Wong, H. C. Man, and F. T. Cheng, 2009, "Effect of pH on Corrosion Behavior of CuCrZr in Solution without and with NaCl," *Journal of Nuclear Materials*, Vol. 394, pp. 52–62.

Kugel, H. W., G. Ascione, S. Elwood, J. Gilbert, and K. Rule, 1996, "Status of Tokamak Fusion Test Reactor Neutron Activation," *Fusion Technology*, Vol. 30, pp. 1065–068.

Lahm, C. E., et al., 1993, "Experience with Advanced Driver Fuels in EBR-II," *Journal of Nuclear Materials*, Vol. 204, pp. 119–123.

Lauridsen, K., P. Christensen, and H. E. Kongso, 1996, "Assessment of the Reliability of Robotic Systems for Use in Radiation Environments," *Reliability Engineering and System Safety*, Vol. 53, pp. 265–276.

Lewis, R. O., 1999, *A White Paper Review: History of Use and Performance of Copper Tube for Potable Water Service*, Lewis Engineering and Consulting, Inc., July, available at www.nuflowtech.com/LinkClick.aspx?fileticket=_TUSCJOCYbc=&tabid=86 and http://www.wsscwater.com/home/jsp/content/pinholescroll.faces?pgurl=/EngAndConst/copperpipewp.html

Lipa, M., A. Durocher, R. Tivey, Th. Huber, B. Schedler, and J. Wiegert, 2005, "The Use of Copper Alloy CuCrZr as a Structural Material for Actively Cooled Plasma Facing and In Vessel Components," *Fusion Engineering and Design*, Vol. 75–79, pp. 469–473.

Liptakova, T., P. Fajnor, and A. Dodek, 2010, "Evaluation of the Flow Accelerated Corrosion of Copper Pipes," *Materials Engineering*, Vol. 17, pp. 7–13.

Ma, B. M., 1983, *Nuclear Reactor Materials and Applications*, New York: Van Nostrand Reinhold, pp. 88–89.

Machalek, M. D., 1983, "First Plasma Operation of TFTR," *Nuclear Technology/Fusion*, Vol. 4, pp. 191–193.

Magaud, Ph., P. Monier-Garbet, J. M. Travere, and A. Grosman, 2007, "Actively Cooled Plasma Facing Components in Tore Supra: From Material and Design to Operation," *Journal of Nuclear Materials*, Vol. 362, pp. 174–180.

Marshall, T. D., and L. C. Cadwallader, 1994, *In-Vessel ITER Tubing Failure Rates for Selected Materials and Coolants*, EGG-FSP-10928, Idaho National Engineering Laboratory, March.

Martin, G., A. le Luyer, F. Saint-Laurent, 2001, "Material Activation Observation on the Tore Supra Tokamak," *Fusion Engineering and Design*, Vol. 58–59, pp. 973–979.

Martinez, J.-M., 2012, *Load Specification for the ITER Vacuum Vessel*, ITER Document 2F52JY, August, Section 1.7.

Masche, G., 1971, *Systems Summary of a Westinghouse Pressurized Water Reactor Nuclear Power Plant*, Westinghouse Electric Corporation, Section 3.4.

NASA, 1971, *Saturn Component Failure Rates and Failure Rate Modifiers*, NASA TM X-64619, National Aeronautics and Space Administration, December.

Neumeyer, C., et al., 2011, "Design of the ITER In-Vessel Coils," *Fusion Science and Technology*, Vol. 60, pp. 95–99.

NRC, 2003, *Reactor Concepts Manual*, U.S. Nuclear Regulatory Commission Technical Training Center, ML023020519, pg. 4–12.

NRC, 1975, *Reactor Safety Study, An Assessment of Accident Risks in U.S. Commercial Nuclear Power Plants*, WASH-1400, NUREG-75/014, U.S. Nuclear Regulatory Commission, October, Appendix III.

O'Connor, P. D., and T. O'Connor, 1985, *Practical Reliability Engineering, second edition*, New York: John Wiley & Sons, Appendix 3.

Oldham, T. R., et al., 2011, "Effect of Radiation Exposure on the Retention of Commercial NAND Flash Memory," *IEEE Transactions on Nuclear Science*, Vol. 58, pp. 2904–2910.

Oldham, T. R., et al., 2009, "Effect of Radiation Exposure on the Endurance of Commercial NAND Flash Memory," *IEEE Transactions on Nuclear Science*, Vol. 56, pp. 3280–3284.

Palmer, D. A., and P. Benezeth, 2004, "Solubility of Copper Oxides in Water and Steam," *Proceedings of the 14th International Conference on the Properties of Water and Steam, Kyoto, Japan, August 29– September 3, 2004*, pp. 491–496.

Perry, W.H., G. L. Lentz, W. J. Richardson, and G. C. Wolz, 1982, "Seventeen Years of LMFBR Experience: Experimental Breeder Reactor-II," *American Power Conference on Nuclear Regulation Future Directions, Chicago, Illinois, April 26–28, 1982,* CONF-820465-2.

Perry, W. H., J. D. Leman, G. L. Lentz, K. J. Longua, W. H. Olson, J. A. Shields, and G. C. Wolz, 1978, "EBR-II: Summary of Operating Experience," *Seminar on Plant Engineering, Mito, Japan, September 20–22, 1978,* CONF-780963-1.

Prince, R., 2012, *Radiation Protection at Light Water Reactors*, Heidelberg, Germany: Springer-Verlag, pp. 16–19.

Reddan, W. G., 1982, "Design and Fabrication of the Vacuum Vessel for the Tokamak Fusion Test Reactor," *Journal of Vacuum Science and Technology*, Vol. 20, pp. 1173–1176.

Sabado, M., and R. Little, 1984, "TFTR Materials Issues and Problems during Design and Construction," *Journal of Nuclear Materials*, Vol. 122&123, pp. 1087–1098.

Samaille, F., M. Chantant, D. van Houtte, J. J. Cordier, and L. Gargiulo, 2005, "Management of a Water Leak on Actively Cooled Fusion Devices," *Fusion Engineering and Design*, Vol. 75–79, pp. 577–581.

Sato, K., 1977, "Flow Induced Vibration Studies for LMFBR in Japan: Past and Recent Studies of FIV for JOYO and MONJU," *Summary Report from the Specialists Meeting on LMFBR Flow Induced Vibrations, IAEA-IGWR Specialists' Meeting on LMFBR Flow Induced Vibrations, Argonne, Illinois, September 20–23 1977,* INIS reference number 32011768.

Sawan, M., 2012, *Model and Analysis of Results for Lower VS and ELM Coils behind BM17 and BM18 at Different Sections*, ITER document number ITER_D_AFLSWJ v1.0, July 18.

Scherpelz, R. I., and J. E. Tanner, 2002, "Neutron Measurements at Nuclear Power Reactors [55]," *Nuclear Instruments and Methods in Physics Research Section A*, Vol. 476, pp. 400–404.

Schlosser, J., et al., 1998, "Design, Fabrication and Testing of an Improved High Heat Flux Element, Experience Feedback on Steady State Plasma Facing Components in Tore Supra," *Fusion Engineering and Design*, Vol. 39–40, pp. 235–240.

Schnauder, H., et al., 1997, "Comparative Availability Analysis of the Four European DEMO Blanket Concepts in View of the Selection Exercise," *Fusion Engineering and Design*, Vol. 36, pp. 343–365.

Schweitzer, P. A., 2003, *Metallic Materials: Physical, Mechanical, and Corrosion Properties*, New York: Marcel Dekker, Inc., Chapter 15.

Seidel, B. R., and R. E. Einziger, 1977, "In-Reactor Cladding Breach of EBR-II Driver-Fuel Elements," *Proceedings of the International Conference on Radiation Effects in Breeder Reactor Structural Materials, Scottsdale, Arizona, June 19–23, 1977*, American Institute of Mining, Metallurgical, and Petroleum Engineers, pp. 139–158.

Shah, V. N., and P. E. MacDonald, 1993, *Aging and Life Extension of Major Light Water Reactor Components*, Amsterdam: Elsevier Science Publishers, Chapter 15.

Smith, G. E., and W. F. B. Punchard, 1977, "TFTR Toroidal Field Coil Design," *Proceedings of the 7th Symposium on Engineering Problems of Fusion Research, Knoxville, Tennessee, October 25–28, 1977*, IEEE, pp. 15–19.

Smith, C. L., V. N. Shah, T. Kao, and G. Apostolakis, 2001, *Incorporating Aging Effects into Probabilistic Risk Assessment—A Feasibility Study Utilizing Reliability Physics Models*, NUREG/CR-5632, U.S. Nuclear Regulatory Commission, Chapter 5 and Appendix A-6.

Stevenson, C. E., 1987, *The EBR-II Fuel Cycle Story*, La Grange Park, Illinois: American Nuclear Society, Chapters 1, 8, and epilogue.

Tatone, O. S., and R. L. Tapping, 1989, "Steam Generator Tube Performance: Experience with Water-Cooled Nuclear Power Reactors during 1985," *Nuclear Safety*, Vol. 30, pp. 382–399.

Thomas, H. M., 1981, "Pipe and Vessel Failure Probability," *Reliability Engineering*, Vol. 2, pp. 83–124.

Tobias, J. B., 1979, "Brazing of Large Section Water-Cooled Copper Conductor on TFTR," *Proceedings of the 8th Symposium on Engineering Problems of Fusion Research, San Francisco, California, November 13–16, 1979*, IEEE, pp. 117–123.

Tsoulfanidis, N., 1983, *Measurement and Detection of Radiation*, New York: McGraw-Hill Book Company, pp. 492, 495.

U.S. Department of Defense, 2002, *Test Method Standard, Electronic and Electrical Component Parts*, MIL-STD-202G, February.

Vallet, J. C., 2007, *Draft Final Report on the Analysis In-Vessel Water Leaks Occurring in Tore Supra*, CETS/NTT-2007-003, Task EDFA TW6-TSL-004, October.

Vanderhoff, J. F., G. V. Rao, and A. Stein, 2012, "Flow Accelerated Erosion-Corrosion (FAC) Considerations for Secondary Side Piping in the AP1000 Nuclear Power Plant Design," *Proceedings of the International Congress on Advances in Nuclear Power Plants (ICAPP-2012), Chicago, Illinois, June 2012*, American Nuclear Society, pp. 2695–2702.

Vandermeulen, W., 1986, "The Effect of Irradiation at 150 and 300°C on the Tensile Properties of Cu and CuCrZr," *Proceedings of the 14th Symposium on Fusion Technology, Avignon, France, September 8–12, 1986*, Oxford: Pergamon Press, pp. 1031–1035.

von Halle, A., and the TFTR Group, 1998, "Final Operations of the Tokamak Fusion Test Reactor (TFTR)," *Proceedings of the 17th Symposium on Fusion Engineering, San Diego, California, October 6–10, 1997*, IEEE, pp. 65–69.

van Houtte, D., et al., 1997, "Availability Analysis of Five Years of Operation of the Superconducting Tokamak Tore Supra," *Fusion Technology 1996: Proceedings of the 19th Symposium on Fusion Technology, Lisbon, Portugal, 16-20 September 1996*, Amsterdam: Elsevier Science, pp. 969–972.

Walters, L. C., 1999, "Thirty Years of Fuels and Materials Information from EBR-II," *Journal of Nuclear Materials*, Vol 270, pp. 39–48.

Walton, G. R., A. Brooks, A. Harnsberger, H. Murray, and J. Satkofsky, 1994, "Design of the TFTR TF Coil Alternate Cooling System," *Proceedings of the 15th Symposium on Fusion Engineering, Hyannis, Massachusetts, October 11–15, 1993*, IEEE, pp. 325–328.

Wiffen, F. W., 1978, *The Response of Inconel 600 to Simulated Fusion Reactor Irradiation*, CONF-7807220017, Oak Ridge National Laboratory, September 8.

Wowk, V., 1991, *Machinery Vibration*, New York: McGraw-Hill Book Company, pp. 275–279.

Wright, R. E., J. A. Steverson, and W. F. Zuroff, 1987, *Pipe Break Frequency Estimation for Nuclear Power Plants*, NUREG/CR-4407, U.S. Nuclear Regulatory Commission, May, pg. B-8.

Wulpi, D. J., 1985, *Understanding How Components Fail*, Materials Park, Ohio: ASM International, Chapter 11.

Zatz, I. J., 2003, *TFTR D&D Project: Final Examination and Testing of the TFTR TF-Coils*, PPPL-3777, Princeton Plasma Physics Laboratory, January.

Zheng, J. H., W. F. Bogaerts, and P. Lorenzetto, 2002, "Erosion-Corrosion Tests on ITER Copper Alloys in High Temperature Water Circuit with Incident Heat Flux," *Fusion Engineering and Design*, Vol. 61–62, pp. 649–657.

Zinkle, S. J., and J. T. Busby, 2009, "Structural Materials for Fission and Fusion Energy," *Materials Today*, Vol. 12, November, pp. 12–19.

Zinkle, S. J., M. Victoria, and K. Abe, 2002, "Scientific and Engineering Advances from Fusion Materials R&D," *Journal of Nuclear Materials*, Vol. 307–311, pp. 31–42.

Zinkle, S. J., 1992, "A Brief Review of Radiation-Induced Cavity Swelling and Hardening in Copper and Copper Alloys," *Proceedings of the 15th International Symposium on Effects of Radiation on Materials*, ASTM STP 1125, American Society for Testing and Materials, pp. 813–834.